Detecting land cover change related to smallholder oil palm plantations:

An automated approach based on multi-temporal Landsat imagery

DITTE MARIE TROJABORG
June, 2017

SUPERVISORS:
Dr. I. C. van Duren
Dr. ir. A. Vrieling
Dr. Mohammad Abdel-Razek (External)

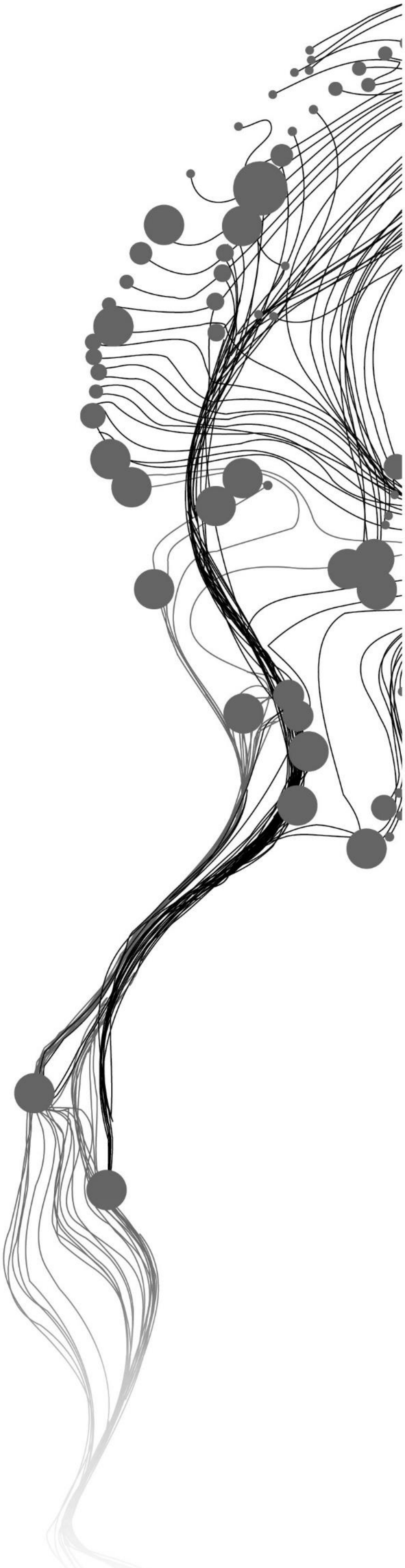

Detecting land cover change related to smallholder oil palm plantations:

An automated approach based on multi-temporal Landsat imagery

DITTE MARIE TROJABORG

Enschede, The Netherlands, June, 2017

Thesis submitted to the Faculty of Geo-Information Science and Earth Observation of the University of Twente in partial fulfilment of the requirements for the degree of Master of Science in Geo-information Science and Earth Observation.
Specialization: Geo-information Science and Earth Observation for Environmental Modelling and Management

SUPERVISORS:
Dr. I. C. van Duren
Dr. ir. A. Vrieling
Dr. Mohammad Abdel-Razek (External)

THESIS ASSESSMENT BOARD:
Prof. dr. A.K. Skidmore
Dr. Ing. Christine Pohl (Universität Osnabrück - Germany)

Abstract

The increasing demand for palm oil is one of the leading causes of deforestation in South-East Asia. The expansion of oil palm plantations has led to serious environmental concerns, such as land degradation and loss of biodiversity. These concerns gave rise to a demand for increased sustainability and transparency in the industry. However, due to poor governance this task is particularly challenging regarding smallholder oil palm plantations (SHOPPs). In recent years, several organizations have emerged to provide sustainability certifications to farmers and farmer cooperatives. To ascertain compliance with sustainability standards, certification organizations often rely on remote sensing tools for monitoring changes in land cover. However, detecting conversions related to SHOPPs in the tropics is challenging since high resolution imagery is expensive and comes at the cost of the temporal resolution necessary for time-series based change detection. While medium resolution imagery has been proven useful in detecting smallholders, missing data due to cloud cover remains an issue. There is consequently a need for feasible and economically viable methods. The purpose of this study is to detect the timing and location of deforestation related to SHOPP establishment or expansion, based on freely available data and open source software. For this study, multi-temporal Landsat TM/ETM+/OLI NDMI time-series data covering the years 2000 – 2016 for the Riau Province in Indonesia was used.

The detection methods of this study are based on the Bfast Monitor near real-time change detection method. To employ Bfast Monitor for historical change detection, it was applied iteratively to the time-series in a sequential manner, whereby for each iteration the monitoring period was limited to one year, from which the breakpoint of the time-series was detected. Decision rules were applied on the outputs of each iteration, so the most likely breakpoints were obtained. To select the most relevant breakpoint per location in the time series, two different approaches are tested: *NDMI Threshold* and *⊿NDMI*. *NDMI Threshold* defines a threshold, below which, a breakpoint is considered more likely to be true. *⊿NDMI* takes advantage of the difference between the land cover present before and after the breakpoint, to determine the likelihood of true change. The results of the spatially applied methods show a similar performance based on their overall accuracies, 74.6% and 76.3%, respectively, for all types of land cover change. In the category of deforestation alone, the methods achieved the overall accuracy of 92.4% and 88.3%, respectively. A probability map of the study area was constructed from the *⊿NDMI* method, whereby larger values for *⊿NDMI* were related to higher probabilities of correctly-predicted land cover change, which was assessed from multi-temporal high-resolution Google Earth imagery. The lowest *⊿NDMI* value (i.e., 0.0) still related to a relatively large probability of ~73%, indicating that Bfast Monitor could effectively limit the detection of breakpoint not related to land cover change.

Both presented methods achieved similar accuracies, however comparing the advantages and limitations of each method, it was concluded that the *⊿NDMI* method is the more promising tool for use in the workflow of certification of smallholder plantations. The method provides an initial framework to assess land cover change and its timing, which has potential to be applied automatically over large areas. However further studies are necessary before a complete integration into certification procedures is possible. Priority needs to be given to testing the robustness of the method at different locations in the tropical region, as well as at larger scales.

Keywords: Smallholder oil palm plantations, sustainability certification, time-series analysis, land cover change detection, Bfast Monitor

ACKNOWLEDGEMENTS

First I want to express my deep gratitude towards my first supervisor Dr. Iris van Duren for her support and dedication throughout this process, without which this project would not have been possible. Also particularly for the constant encouragement, motivation and always having an open door. I would especially like to thank her for her much appreciated personal dedication to my project which gave me extraordinary opportunities and highly valued experiences.

I also want to thank my second supervisor Dr. ir. Anton Vrieling, for providing much appreciated ideas, discussion and insight.

I want to especially express my gratitude towards ISCC and GRAS, for the opportunity to work with them, it was a valuable experience, which inspired and motivated me for this project. A special thanks to my external supervisor Dr. Mohammad Abdel-Razek for his invaluable help and advice in particularly challenging parts of my research, as well as his warm welcome, support and assistance throughout my stay with ISCC. Also a special thanks to all my colleagues in Köln who welcomed and included me and provided much needed assistance in all the practical challenges of my internship.

I would like to acknowledge the advice provided by Dr. Ing. Christine Pohl, and thank her for inviting me to visit University of Osnabrück, which was an appreciated learning experience, even though my research finally went into a different direction.

I also want to acknowledge the staff of Geo Centrum, Lund University for making the first year of the GEM program, a good and valuable experience with their motivation and dedication to this field. A special thanks to Prof. Dr. Petter Pilesjö for greatly appreciated help and advice in practical challenges related to the GEM program.

Finally I would like to dedicate this thesis to my family and friends, who provided me with all the support I needed during these challenging two years away from home.

Table of Contents

LIST OF FIGURES

LIST OF TABLES

1 Introduction

1.1 Background

1.1.1 Oil palm production and certification

The production of palm oil has expanded significantly in recent times. The oil palm industry is the most profitable agricultural sector in the tropics and the global demand for palm oil is expected to increase as the global population increases (Sayer et al., 2012). Palm oil has a wide range of applications ranging from food and cosmetics to biofuel. It has become especially attractive as a potential renewable energy source due to its low production costs and high yields (Tan et al., 2009).

The production of palm oil takes place in regions such as South America, Africa and South-East Asia, which provide the humid, tropical climate suitable for oil palm cultivation (Verheye, 2010). Since 2006, Indonesia has taken the place as the world's leading producer of palm oil (Block, 2013), and oil palm is now the main contributor to Indonesia's gross domestic product in the agricultural sector (Nurdiana et al., 2016). Furthermore, according to the Indonesian government, the extent of oil palm plantations is expected to increase from approx. 7 million ha in 2009 to 10-12 million ha by 2020 (Bahroeny, 2009). Projections based on provincial plans for Indonesia estimates that the increase in acreage will be 10.7% annually until 2020 (Wicke et al., 2011).

The impacts of the palm oil industry are extensive in the economic, social and environmental sectors of Indonesia. According to Sayer et al., (2012), the increasing size of the industry brings economic value to the country, but with complex consequences for the local population. While an increase in production brings more employment opportunities in large companies, the local rural population often does not benefit from this, since the companies prefer to employ foreign work force with the proper work experience (Sayer et al., 2012).

As a solution, Sayer et al. (2012) concluded that adopting smallholder plantations can be a viable way of income for many rural farmers, to improve their livelihoods and reduce poverty. Local farmers are therefore encouraged to develop Smallholder Oil Palm Plantations (SHOPPs) (Rist et al., (2010), and due to poor governance, farmers now manage the establishment and expansion of their plantations independently (Euler et al., 2015).

Other side effects of the expanding oil palm industry consist of serious negative consequences for the environment, including deforestation, land degradation, forest fires, loss of biodiversity and peatland destruction (Tan et al., 2009). As the demand for palm oil increases, so does the demand for arable land to expand oil palm production. While studies show that oil palm expansion can be sustainable (Wicke et al., 2011), the decisions on where to establish plantations are based on economic rather than environmental concern (Sayer et al., 2012). According to Miettinen et al., (2012), South East Asia has experienced a significant decline in peatland areas due to extensive deforestation. In peninsular Malaysia, Sumatra and Borneo, the extent of peat swamp forests has been reduced from 76 % in 1990 to 29 % in

2015 and 73 % of the industrial areas are accounted for by oil palm plantations in 2015 (Miettinen et al., 2016). The authors predict that by 2030, all peatlands will disappear from the region if deforestation continues at the current rate.

Deforestation of peatlands caused by oil palm plantation establishment is a serious global environmental issue as it results in substantial amounts of carbon being released to the atmosphere through peatland fires and peat oxidation as a result of drainage, a common practice in oil palm cultivation (Koh et al., 2011; Nurdiana et al., 2016; Uryu et al., 2008). Economically viable methods of monitoring SHOPP developments are therefore essential to ensure environmental and social sustainability (Environmental Investigation Agency, 2014). The Indonesian government and NGOs agree that mapping the development of smallholder plantations and ensuring public availability of data are the keys to ensure sustainability of the Indonesian palm oil industry (Lake, 2016).

Several certification organizations (e.g. ISCC, RSPO) assists in monitoring the production chain, to uphold the standards of sustainability in the sector, according to defined criteria. The importance of certification in the industry is supported by Barry et al. (2012), who showed that certification schemes have a positive influence on both social and environmental practices. Among others, ISCC (International Sustainability and Carbon Certification) provides certification systems to the palm oil industry and specializes in certifying sustainable palm oil in the biofuels-industry. As an independent third party certification system, ISCC ensures sustainability on different levels, such as climate change mitigation and the protection of biodiversity, the environment and human rights (ISCC, 2016). According to the report on sustainability requirements formulated by ISCC, the production of biomass for biofuel needs to comply with certain criteria to qualify for the ISCC certificate (ISCC, 2011). To confirm that sustainability requirements are met, the location, timing and extent of land cover conversions into oil palm plantations need to be monitored. According to ISCC's sustainability requirements, oil palm cannot be produced on land with a high biodiversity value or high carbon stock. Oil palm plantations cannot be certified if they were established on peatlands before January 2008, the cut-off date defined by ISCC (ISCC, 2011).

1.1.2 Remote sensing application: land cover change detection

Remote sensing has been used extensively and successfully to monitor the spatial distribution of crop lands and other vegetation land covers (Xie et al., 2008). Previous studies related to oil palm were often focused on detecting industrial plantations (> 50 ha) with different classification approaches and data sources (e. g. Nooni et al., 2014; Petersen et al., 2016). In the often-cloudy tropical regions, multiple observations are required to obtain useful and timely information on land cover changes (Carlson et al., 2012; Miettinen et al., 2012) and commonly-used optical data sources therefore include multi-temporal MODIS (Koh et al., 2011), and Landsat imagery (Gunarso et al., 2013).

Several studies have been conducted to determine land cover changes related to large-scale oil palm plantations, mainly by applying bi-temporal optical imagery and applying a post – classification change detection approach (Darma et al, 2015; Gunarso et al., 2013; Ramdani & Hino, 2013). Others have incorporated time-series analysis based on Vegetation Indices (VI) in order to detect the timing of land cover disturbances (e.g. Broich et al., 2011; DeVries et al., 2015; Gutiérrez-Vélez & DeFries, 2013). The work of GRAS (Global Risk Assessment Services) has shown time-series plots based on MODIS derived

EVI (Enhanced Vegetation Index) to be efficient in detecting large scale changes in oil palm plantation (GRAS - Global Risk Assesment Services, 2015).

Limited research has been conducted related to land cover conversions caused by the establishment of SHOPPs, as studies often focus on the economic and social aspects of smallholder development (e.g. Rist et al., 2010; Sayer et al., 2012). SHOPPs are defined as covering less than 50 ha (RSPO, 2016) and can therefore be challenging to detect with remotely sensed data. The frequent cloud coverage in tropical regions complicates this task further (Asner, 2001). Remotely sensed data with a high temporal resolution (e. g. MODIS and Landsat) is widely available, but comes at the cost of spatial resolution. Successful approaches so far has been few and diverse. Miettinen et al. (2016) included SHOPPs in their land cover distribution studies of South-East Asia using multi-temporal Landsat imagery. Gutiérrez-Vélez & DeFries (2013) used Landsat combined with SAR imagery to quantify the areas converted into SHOPPs in South-America, while Yayusman & Nagasawa (2015) relied on SAR imagery alone to detect SHOPPs in Indonesia. DeVries et al. (2015) used the Bfast Monitor method for time-series based, small-scale disturbance detection of tropical forests in Ethiopia.

1.1.3 Theoretical background: Breaks For Additive Season and Trend

This study implements the Bfast (Breaks For Additive Season And Trend) Monitor near real-time land cover change detection method, which was developed by Verbesselt et al. (2012), as an extended approach based on the Bfast-algorithm (Verbesselt et al., 2010a). The Bfast-algorithm has been used in different studies for the purpose of change detection or land cover monitoring in various locations (e.g. DeVries et al., 2015; Hamunyela et al., 2016; Schultz et al., 2016) and was created as a generic, data-driven change detection method for time-series analysis. Bfast generally works by decomposing the time-series into trend, seasonal and remainder components and has proven robust in handling datasets affected by outliers and data gaps (i.e. missing data) (Verbesselt et al., 2012). According to Verbesselt et al., (2010b), the method was constructed to handle the three types of change, characteristic of terrestrial plant ecosystems: 1) phenological change, 2) abrupt change and 3) gradual change.

Bfast Monitor was originally developed to provide a monitoring system for newly acquired satellite data (Verbesselt et al., 2012), nonetheless it has also been proven a robust method for historical change detection (DeVries et al., 2015a, 2015b; Dutrieux et al., 2016). The method works by modelling the identified stable historical variation of the time-series. According to Verbesselt et al. (2012), this makes detection of structural land cover change possible by identifying when the model is no longer stable for new data. To implement Bfast Monitor, some concepts need to be described, which are summarized in Table 1.

Table 1: Concepts used in implementing Bfast Monitor.

Concepts	Description
Breakpoint	Identified moment of land cover change
Historical-period	Time-period before the breakpoint, used to model the stable vegetation dynamics
Magnitude	The magnitude of the breakpoint. Defined as the median of the residuals in the monitoring-period
Monitoring-period	Time-period for which the algorithm looks for a breakpoint in the data
Start Date	Start date of the monitoring-period

First step of employing the method, is to define the historical-period and the monitoring-period. The historical-period describes the stable time-period of a time-series (i.e. with stable data variation) of previously acquired data. An example is given in Figure 1, where the historical-period is shown to contain the historical data and stable history. A regression model of the trend and seasonal components of the time-series, is fit to the data points of the historical-period to model the vegetation dynamics of the stable period (Verbesselt et al., 2012). As described by Verbesselt et al. (2012), the start of the stable historical-period is identified by expert-knowledge or automatically. The end of the historical-period is defined by the start of the monitoring-period, set by the "Start Date", as illustrated in Figure 1. The monitoring-period defines the time-period of newly acquired data, where the moment of land cover change is detected, i.e. it is the period being monitored for disturbances. The "Start Date" (start of monitoring-period) is set by the timing of newly acquired data or by expert-knowledge, since it should be set before any likely disturbance, otherwise the disturbance will not be detected in the monitoring-period. The moment of disturbance in land cover change (labelled as "breakpoint", figure 1) is detected in the monitoring-period, when a structural change is registered in the new data, compared to the stable trend and seasonal components modelled in the historical-period (Verbesselt et al., 2012). A Magnitude is assigned the detected breakpoint by finding the median of the residuals of the modelled values and the new data of the monitoring-period (DeVries et al., 2015a).

Several freely available tools were created by Dutrieux et al. (2017) based on Bfast Monitor in the open source software R. The tools were made for a spatial implementation of Bfast Monitor, and the main functions are Bfm Pixel and Bfm Spatial, which are applied to a single pixel or to every pixel of a raster, respectively. A breakpoint (if any) and the Magnitude is reported for Bfm Pixel, and a raster stack consisting of a breakpoint layer and a Magnitude layers is the result of Bfm Spatial. The breakpoint(s) can be filtered by applying a Magnitude threshold to avoid false breakpoints (Dutrieux et al., 2017), however the threshold is highly dependent on the study area and should be set based on expert-knowledge or ground truth data (DeVries et al., 2015).

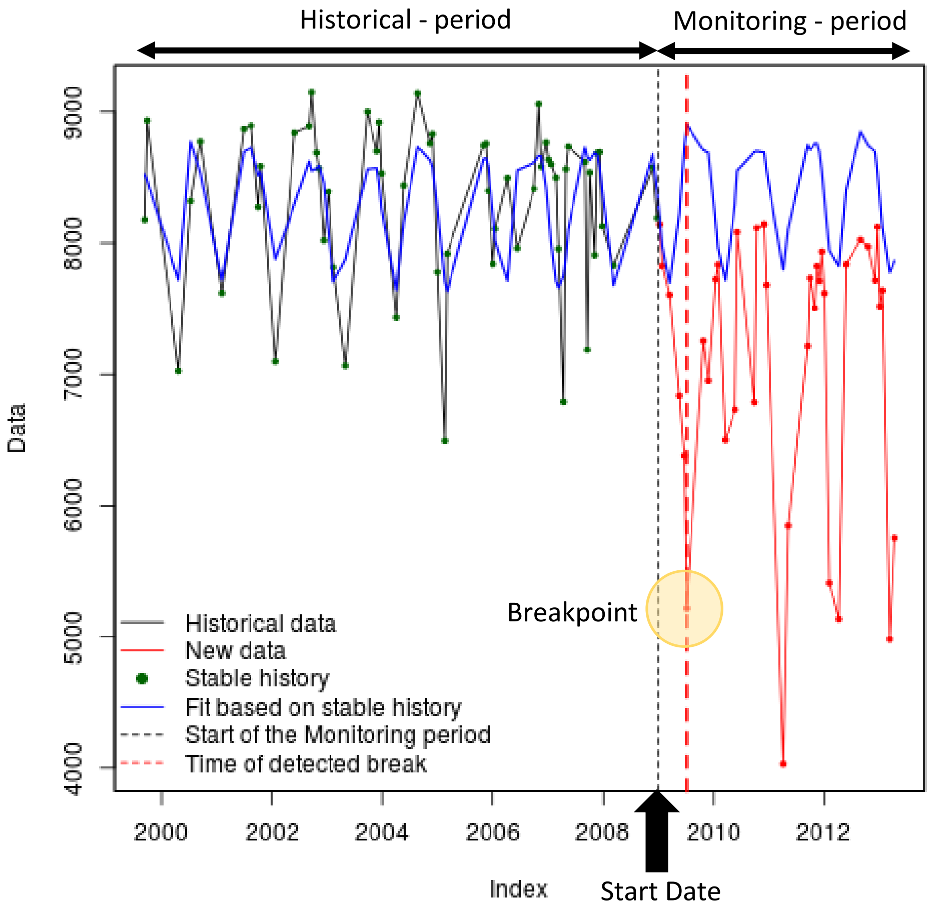

Figure 1: Illustration of the concepts of Bfast Monitor, modified from Dutrieux et al. (2017). The illustration is based on a single pixel analysis with Landsat NDVI. The concepts of historical-period and monitoring-period are illustrated above the figure, with arrows indicating their location along the time-line (i.e. 2000 – 2013). The historical-period includes the historical data and stable history (black line with green points). The monitoring-period includes the newly acquired data (red line and points) and the detected breakpoint (yellow circle), with the timing of the detected breakpoint, illustrated by the red dashed line. The end of the historical-period and start of the monitoring period is defined by the "Start Date", illustrated by a black arrow and black dashed line.

1.2 Problem statement

The role of smallholder plantations in the oil palm industry in Indonesia is increasing and likewise are the negative impacts on the environment and the social sector. Monitoring of SHOPPs is essential for certification organizations to ensure that sustainability criteria are met, since reliable information is not easily available. This supports the need for a feasible, economically viable land cover change detection method, which is applicable for historical and near real-time detection, without the need for method-specific expert-knowledge.

In this study, a novel automated land cover change detection approach is presented, which provide the benefits of freely available data and open source software, and does not require method-specific expert-knowledge. The approach relies on Bfast Monitor, which has previously been used for historical, small-scale disturbance detection in tropical areas (DeVries et al., 2015). The term expert-knowledge, in the context of this study, is defined as the knowledge needed to set the parameters of Bfast Monitor, which required in-depth knowledge of the study area or time-series analysis. The goal of this study is to provide a beneficial tool to incorporate in a certification framework, which is not restricted by the study area of this study, but is applicable throughout the humid, tropical regions where oil palm is cultivated.

1.3 Objective and research questions

The main objective of this study is to detect the extent and timing of land cover conversion related to smallholder oil palm plantation establishment or expansion from multi-temporal Landsat imagery.

Based on the main objective, the following research questions are defined:

1. Which vegetation index derived from Landsat shows the strongest temporal response to known land cover conversions related to smallholder oil palm plantation establishment?

2. How can the approximate location and timing of these conversions be automatically extracted from Landsat vegetation index time series?

3. Can the probability of land cover change be mapped for areas identified as potential change areas?

2 Study Area and Data

2.1 Study area: Riau Province, Sumatra, Indonesia

In South East Asia, the largest area of oil palm plantations established on peatlands are found in Sumatra, Indonesia (Gunarso et al., 2013). One of the main oil palm producing areas on Sumatra is located in the Riau Province. Sumatra is also considered to hold the largest carbon storage in Indonesia as well as being home to several endangered species that are dependent on the natural forests in the area (Uryu et al., 2008). According to WWF (World Wildlife Fund) Indonesia, natural forest cover in the province has been reduced by 65 % since the 1980's up to 2008. The Province has one of the highest deforestation rates in Indonesia and has lost more peat swamp forest than any other region (Koh et al., 2011).

The Riau Province has a humid, tropical climate with rainfall of approx. 1000-3000 mm on average, per year, and the climate is characterized by a wet and dry season, with the wet season covering September – March (Ramdani & Hino, 2013).

2.2 Data

Landsat 4/5 TM, 7 ETM+ and 8 OLI imagery was downloaded from USGS for January 1st 2000 – October 15th 2016. Scenes with a maximum of 80 % cloud cover were selected at Level 1TP processing level (i. e. the highest quality products, suitable for time-series analysis at pixel level (USGS, 2017)), resulting in a total of 224 scenes. The images were cropped and resampled by the supplier, USGS. After downloading the datasets, clouds and cloud shadows were masked using the CFMask supplied with the data (USGS, 2017). Next, the masked images were stacked and are then ready for processing. Ancillary land cover maps of Indonesia were provided by WWF Indonesia and GRAS for 2007 and 2009, respectively.

The following three Landsat datasets were downloaded as final VI products: Normalized Difference Vegetation Index (NDVI), Enhanced Vegetation Index (EVI) and Normalized Difference Moisture Index (NDMI). The NDVI and EVI are calculated from the Near Infra-Red (NIR) and Red (R) bands with the following equations:

$$NDVI = \frac{NIR - R}{NIR + R}$$

$$EVI = G * \left(\frac{NIR - R}{NIR + C1 * R - C2 * B + L}\right)$$

where L corrects for the canopy background, C1 and C2 are coefficients for atmospheric resistance and B is the blue band. The additional components of the EVI formula can, in most cases, reduce atmospheric and background noise, and saturation (USGS, 2017).

The NDMI is calculated as the ratio between NIR and Short-Wave Infra-Red (SWIR) (USGS, 2017):

$$NDMI = \frac{NIR - SWIR}{NIR + SWIR}$$

The choice of comparing NDVI, EVI and NDMI in this study was based on three considerations:

- The availability of finished VI products from USGS (USGS, 2017).
- ISCC/GRAS has extensive experience in the field of land cover change detection related to certification purposes. In their work, MODIS-derived EVI was used for larger scale land cover change detection (industrial-sized oil palm plantations). EVI was therefore the obvious choice for testing a Landsat based approach. The NDMI was also already considered for implementation by ISCC/GRASS as a viable approach to oil palm detection.
- The Bfast Monitor near real-time change detection method was developed and tested by the authors by applying a NDVI time-series dataset for time-series based change detection (DeVries et al., 2015; Dutrieux et al., 2017; Dutrieux et al., 2015; Verbesselt et al., 2010; Verbesselt et al., 2012).

2.3 Selecting a test location for method development

To conduct this study, a limited area within the Riau Province was selected for method development and testing, based on Google Earth high resolution imagery. Due to the extensive processing time of a complete spatial analysis, on a full time-series, an area of 5 x 5 km was defined as the specific study area and test-site. Since the objective of this study is to detect land cover change related to SHOPPs, regardless of specific geographical location, the exact study area is of less importance. However, certain criteria were taken into account for selecting a suitable location for the study of small-scale oil palm related land cover change.

Since reliable land cover data is not available for the location of smallholder plantations in Indonesia, it should be possible to visually distinguish SHOPPs from other land cover types in satellite imagery. Visual indicators of SHOPPs are based on the shape and planting patterns of oil palm trees, which can be identified in high resolution satellite imagery (such as Google Earth). Industrial plantations are usually planted in regular, rectangular formations of approx. 25 ha, which are easily visually identified in satellite imagery (Gaveau et al., 2016; Gutiérrez-Vélez & DeFries, 2013). Visually identified oil palm fields, which do not follow the standard planting practices of industrial oil palm plantations (e. g. rectangular or square planting patterns, monocrop practices, optimum tree density and spacing, standard field size of 100 ha rectangular blocks (Verheye, 2010)), are thus considered likely to be SHOPPs (Gutiérrez-Vélez & DeFries, 2013). An example of identified oil palm cultivation that does not follow the industrial standard practices, is shown in Figure 2.

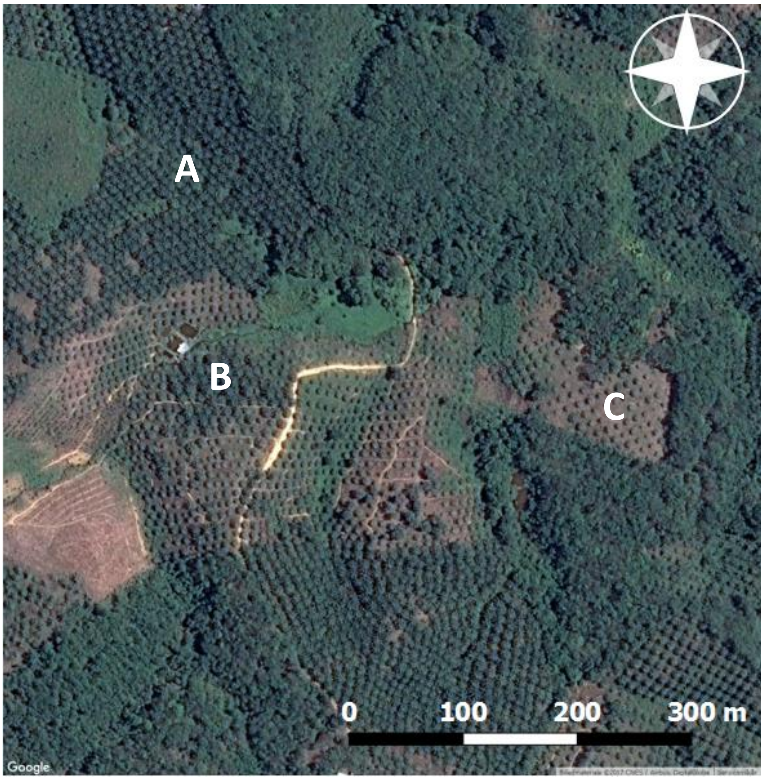

Figure 2: Image of scattered patches of oil palm plantations, identified by the characteristic triangular planting pattern. The patches likely belong to smallholder farmers since the typical rectanguler block shape of 25 ha is not observed (A). Also mixed growing rates can be seen (B), and the size of one patch is relatively small (C).

It is necessary to identify areas that were converted from forest to oil palm plantation, and high resolution imagery should be available in order to validate the type of conversion. It is therefore a criterion that historical Google Earth imagery are available at two points in time.

The criteria for selecting a test site within the study area are the following:

1. The identified oil palm field should be bordering a known SHOPP (based on ancillary maps) or be scattered in patches of irregular size and patterns.
2. Historical Google Earth imagery should be available at two points in time, to determine if land cover change has occurred. Establishment of oil palm plantations should be observed by comparing historical and recent Google Earth imagery.

To select the suitable location, ancillary land cover maps of the region were imported into Google Earth to find locations of known oil palm. Furthermore, a ".kmz" file displaying the Landsat-missions paths and rows globally was imported to select locations within overlaying paths. This way, more Landsat scenes are available for the area, which is highly beneficial in time-series analyses, to reduce the risk of data gaps caused by cloud cover.

Based on implementing the aforementioned two criteria for location selection in a visual study of the Riau Province in Google Earth, Location ID1 was selected as test site (Figure 3). Location ID1 is 5x5 kilometer, the North-West corner is located at 1° 11' 37.94" N and 101° 6' 58.83" E and the South-East corner is located at 1° 8' 55.05" N, 101° 9' 48.97" E. The area was partially covered by registered smallholder plantations in 2007, according to WWF Indonesia. For this location, clear Google Earth historical imagery is available for the year 2006 and 2014.

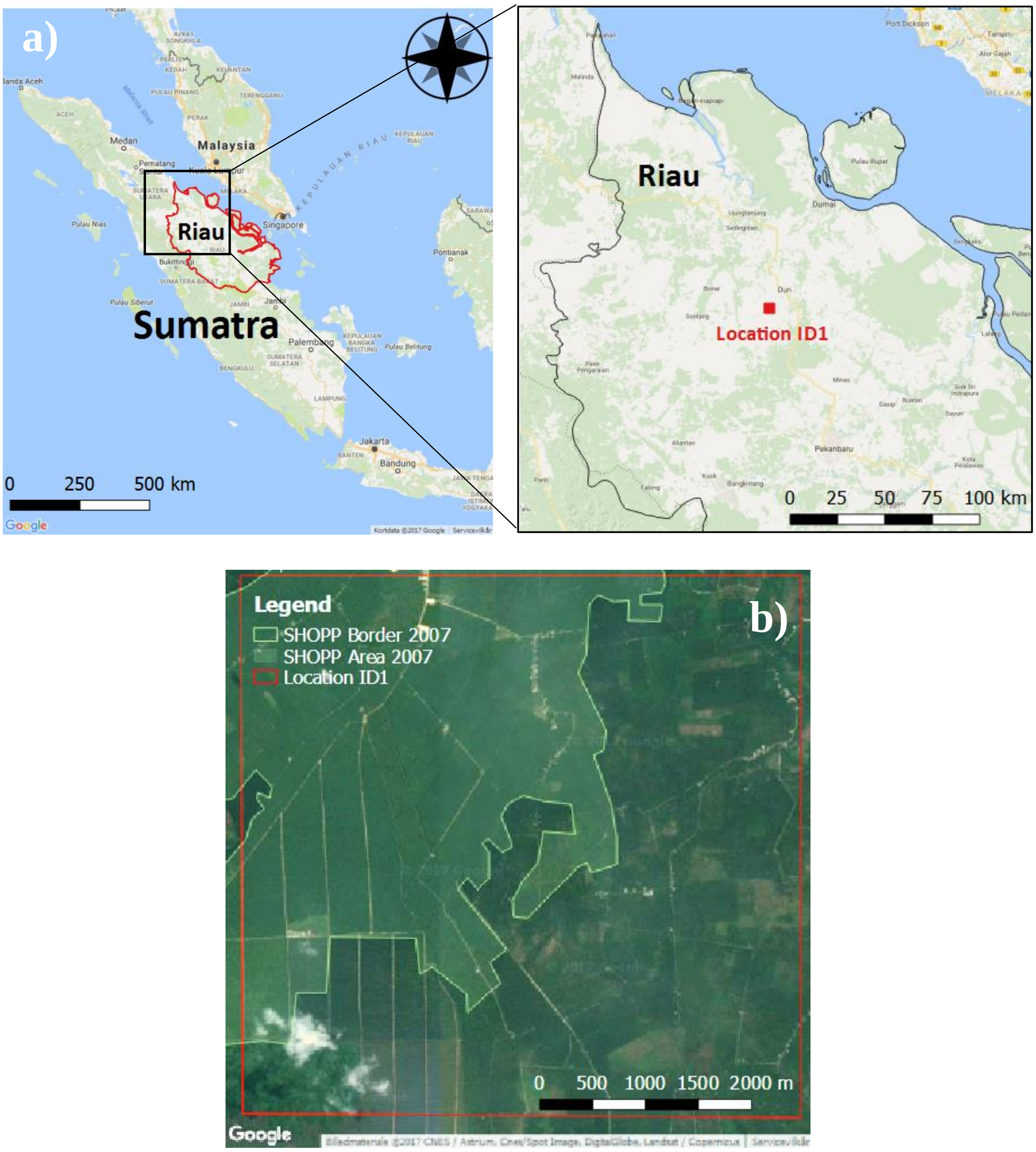

Figure 3: The location of the study area. Location ID1 was selected in the northen part of the Riau Province, located on Sumatra in Indonesia.

3 Methodology

The methodology in this study is designed in three steps to detect the timing and the location of land cover change due to shop establishment using Landsat imagery. The first step is comparison of the performance of VI's to select the most suitable VI based on the defined criteria. The second step is to use the selected VI for spatio-temporal detection of land cover change related to SHOPPs. The third step is to generate a probability map for the detected land cover changes. Figure 4 illustrates the main steps of the methodology of this study.

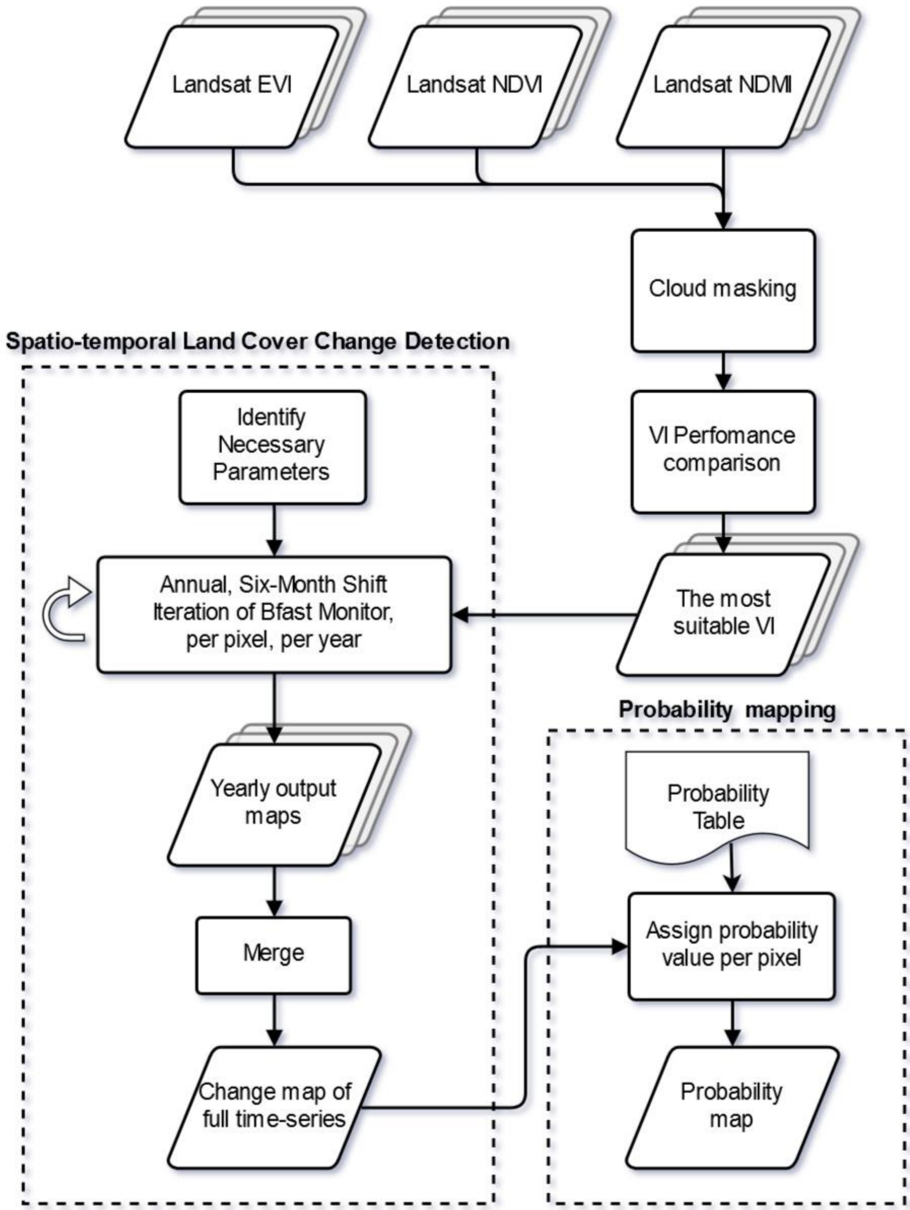

Figure 4: Flowchart illustrating the main steps of this study.

3.1 Comparison of Vegetation Indices

3.1.1 Selection of test-pixels

To assess which Landsat-derived VI shows the strongest response to known forest to oil palm conversions, a number of test-pixels were selected. Within Location ID1, purposively pixels were selected to characterize the temporal signal of each VI, representing:

a) Stable forest and other dense vegetation (including primary, secondary forest, peat swamp forests and non-oil palm plantations)
b) Stable oil palm plantation
c) Land cover change: Stable forest and other dense vegetation → oil palm

Because reliable land cover data were not available, the three classes were identified based on the mean VI values at different time intervals for each of the VI's. Figure 5 shows the mean values of the full time-series: year 2000 – 2016. Intermediate mean values (yellow) resulted from either consistent intermediate VI values or a combination of small and large values (e. g. due to land cover change). The spatial variability in NDVI is smaller as compared to EVI and NDMI (Figure 5). The majority of pixels has high NDVI values, making different land cover patches difficult to visually distinguish from each other. According to figure 5c, the range and distribution of NDMI values makes it possible to distinguish land cover patches which makes NDMI more beneficial for selecting area of land cover change.

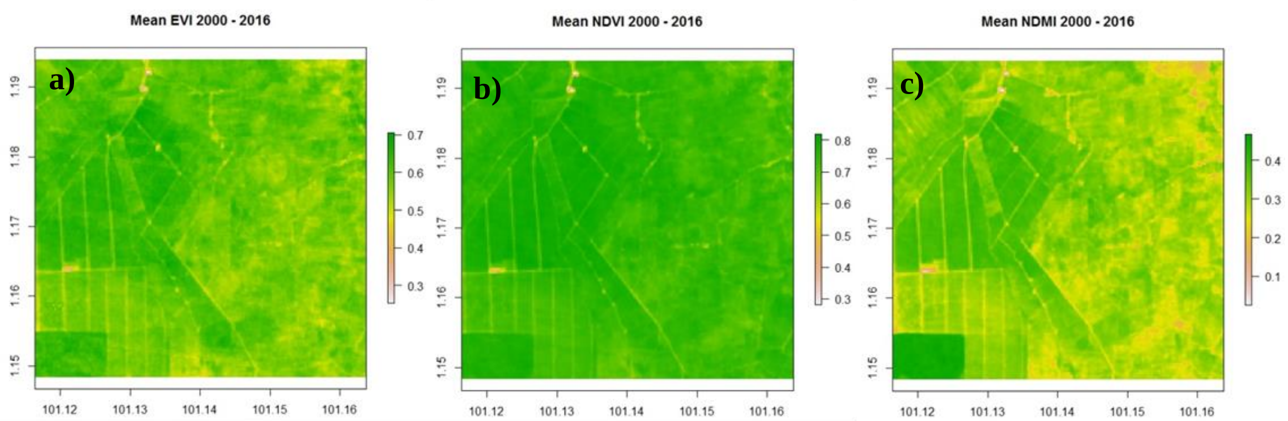

Figure 5: Mean values for the full time-series: 2000 – 2016, Location ID1. A): mean Enhanced Vegetation Index (EVI) values, b): mean Normalized Difference Vegetation Index (NDVI) values, c): mean Normalized Difference Moisture Index values.

The NDMI map as well as newly generated mean value and standard deviation NDMI maps for the period of 2006 – 2014 (see Appendix A) were compared with high resolution Google Earth imagery to visually confirm the location of stable land cover and areas of land cover change. Using the confirmed locations, the following three (GIS) layers were created in order to generate the test-pixels:

- Land Cover Change (stable dense vegetation → oil palm)
- Stable Dense Vegetation
- Stable Oil Palm

The land cover GIS layers were manually digitized based on Google Earth imagery, using the open source GIS software QGIS and the result is shown in Figure 6. Within each GIS layer, test-pixels were generated using stratified random sampling. With this method, the number of random pixels per area is determined based on the proportional size of each area, out of the total area (sum of the three GIS layers). 100 pixels were chosen in total, and the number of pixels within each area were calculated as follows:

$$n_h = \left(\frac{N_h}{N}\right) * n$$

where n_h is the sample size for class h, N_h is the area size for class h, N is the area sum of the classes and n is the total number of samples. The land cover classes, the size of each class and the number of random test-pixels are shown in Table 2. The distribution of the test-pixels is shown in Figure 6.

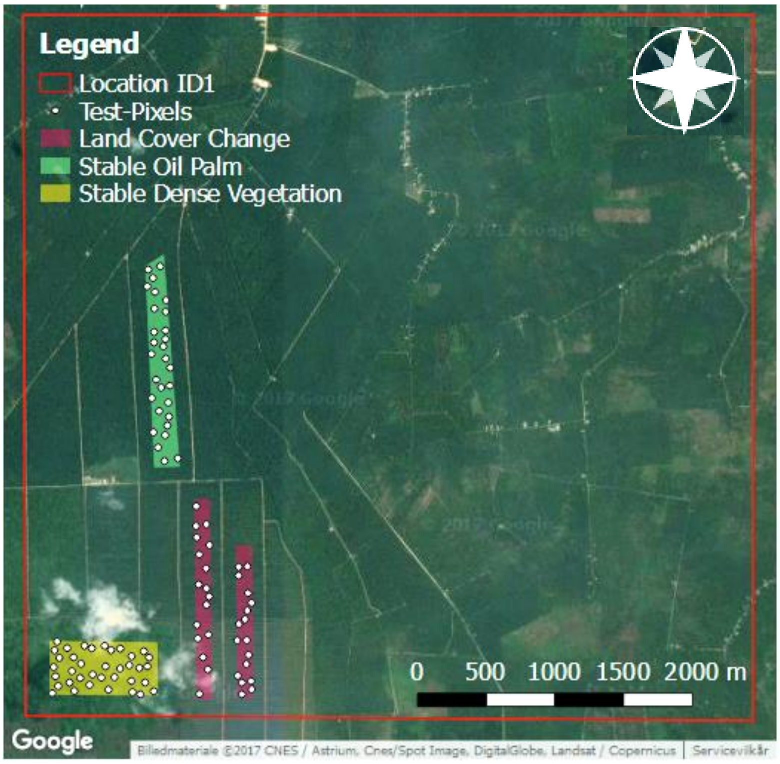

Figure 6: Location of 100 random test-pixels. The 100 test-pixels are distributed within the Land Cover Change, Stable Oil Palm and Stable Dense Vegetation classes.

Table 2: The size and number of random test-pixels for each land cover class.

Land Cover Class	Size in Ha	Number of Random Test-Pixels	Percent out of Total Area
Stable Dense Vegetation	29.5	37	37 %
Stable Oil Palm	23.3	29	29 %
Land Cover Change	27.5	34	34 %

3.1.2 Visual comparison

The three VI's are indicators of the presence of green vegetation, sensitive to either the photosynthesis rate of the canopy (NDVI and EVI) or the canopy moisture content (NDMI). Because of this, land use changes that affect the green vegetation are expected to show up in the time series of these indices. The conversion of forest or other dense vegetation into oil palm would lead to a significant drop in VI values after clearance of the initial vegetation. The following VI values were expected to steadily rise over the next 5 years, the growth period of oil palm (Verheye, 2010). This pattern was expected to be recognizable, particularly because of the absence of distinct seasonal fluctuations in tropical regions, which could otherwise obscure the change pattern. All VI's should be able to portray this pattern, due to their ability to enhance vegetation features (Viña et al., 2011). For the stable land covers, the temporal profiles were expected to have less variation in VI values over time.

To compare the temporal response of each VIs visually, time-series profiles of three random test-pixels of each land cover class were plotted for illustration purposes. Three test-pixels (in total 27) were evaluated as it was not feasible to individually compare 3 x 100 time-series profiles visually, however the full number of test-pixels were used for further analysis.

The visual comparison of the VI time-series profiles followed a qualitative approach. To evaluate the suitability of each VI for further analysis, suitability was defined by the following questions:

- **Question 1.a**: Can a land cover change signature be identified in the temporal signal of the VI, within the Land Cover Change class?
- **Question 1.b**: Can a stable land cover signature be identified in the temporal signal of the VI, within the stable land cover classes?
- **Question 2**: Can the temporal signal of stable land cover or land cover change easily be recognized without interference from outliers?

Based on the suitability questions, each test-pixel was assigned the label "Yes" or "No" in each of the questions. The VI with the most "Yes" labels, was then considered the most suitable index for further analysis.

3.1.3 Comparison of NDVI, EVI and NDMI based on Bfm Pixel test runs

To assess if the visually-identified most suitable index also resulted in an optimal detection of breakpoints based on Bfast, Bfast Monitor was applied to all 100 test-pixels with each of the three VI's. However, before running any Bfast Monitor function, the function parameters need to be defined. The following parameters were set manually, since they are sensitive to the datasets: Formula, start date, and history. The other Bfast Monitor parameters were set to default values based on the advice of the creators of the Bfm Pixel and Spatial functions (Dutrieux et al., 2017).

A random test-pixel from each land cover class was used for parameter setting, and based on interpretation of the time-series profiles, initial assumptions were made about the setting of each parameter:

- The value of "history" determines the length of the historical-period. It was set to include all data points of the historical-period, as this ensures sufficient data for modelling the trend, if data gaps exists (DeVries et al., 2015a).
- By combining information from Google Earth historical imagery and the visually distinguished moment of change in the time-series plots of the Land Cover Change class, change was concluded to have occurred after 2006. Consequently the "Start Date" was set to 2006, Julian day 1.
- The "formula" was set to include modelling of both the trend and seasonal component in the historical-period, to account for any seasonality which might influence the temporal signals.

These parameter settings were used to run Bfm Pixel on each of the three random test-pixels. The parameters were modified for each VI to optimize the output, if the expected breakpoint or absence of breakpoint was not correctly detected by Bfm Pixel.

After setting the parameters, Bfm Pixel was run for the 100 test-pixels with each VI dataset as input. The accuracy of running Bfm Pixel with each VI was determined and compared in order to conclude which VI is suitable for Bfast Monitor time-series analysis. The suitability of a VI dataset was defined by the number of false breakpoints detected by Bfm Pixel, with a given VI as input. False breakpoints were defined as follows:

Detected breakpoint are different than expected breakpoint, i. e.:

- Breakpoint detected for a pixel within the stable land cover classes, where no breakpoint is expected.
- No breakpoint detected within the Land Cover Change class, where a breakpoint is expected.
- Breakpoint detected within the Land Cover Change class, but at a time different than expected.

Each of the 100 test-pixels were analyzed with the Bfm Pixel function, and the outputs were compared. For all the test-pixels in the stable land cover classes, it was expected that no breakpoints were detected, for the Land Cover Change class, a breakpoint for each pixel was expected. For every test-pixel in the Land Cover Change class, the time-series plot was checked visually to determine if the breakpoint was detected at the moment of expected land cover change, or in close proximity (based on the drop in VI values). Finally, the number of false breakpoints detected within each class, and with each VI dataset, were compared.

3.2 Spatio-temporal land cover change detection

An automated change detection method is essential to provide a tool for people with little GIS and remote sensing experience in land cover change detection. The goal of constructing the method is to limit the input knowledge needed from the user as much as possible. The approach presented in this study is based on the Bfast Monitor functions, and the user-defined inputs are limited to: the pre-processed Landsat VI data set, the start year and the end year of the dataset.

3.2.1 Identifying the necessary parameters

First it was necessary to identify parameters of the original Bfast Monitor, which requires expert-knowledge. The "Start Date" of the monitoring-period is set by the user, based on expert-knowledge for historical change detection. The chosen "Start Date" has considerable consequences for the output, as the monitoring-period defines the period during which the Bfast-algorithm will look for a breakpoint (Table 1) (Verbesselt et al., 2012). In Figure 7, the consequences of different "Start Date" settings are demonstrated, based on running Bfm Pixel on a test-pixel from the Land Cover Change class. The NDMI dataset was used as input and three different "Start Date" settings, year 2005, 2007 and 2009 were chosen to illustrate an example. The resulting breakpoints were detected in year 2006, 2007 and 2012 respectively. From the three examples in Figure 7, it can be seen that the chosen "Start Date" affects the modelling of the historical period considerably, which is illustrated by the three different patterns of the blue line in each time-series (Figure 7). Because of this, three different breakpoints resulted for the same input pixel. Furthermore, based on the original dataset, it appears that a significant change within the time-series occurred in 2006, which is shown by the sudden drop in VI values. This observation supports the first detected breakpoint in Figure 7a, in July 2006. However when the "Start Date" is set after 2006, the drop is not recorded as a breakpoint and is included in the modelling of the historical-period.

The original Bfast Monitor was created with the purpose of near real-time change detection (Verbesselt et al., 2012), so the purpose is to analyze one specific time period in recent time, based on one specific "Start Date", known by the user as the first date of the newly acquired data. The "Start Date" can be unknown by if the purpose is historical change detection (e.g. the case of the study by DeVries et al. (2015)). To manually set the correct "Start Date" (i.e. so the monitoring-period includes the breakpoint to be detected) will require the user to have in-depth knowledge of the study area or time-series analysis. Furthermore, when applying Bfast Monitor spatially, the same "Start Date" is applied to every pixel. As the land cover dynamics can differ significantly between any two pixels, using one "Start Date" for every pixel is not preferable in a spatial application. An essential part of the new change detection approach is consequently to circumvent the use of a single "Start Date".

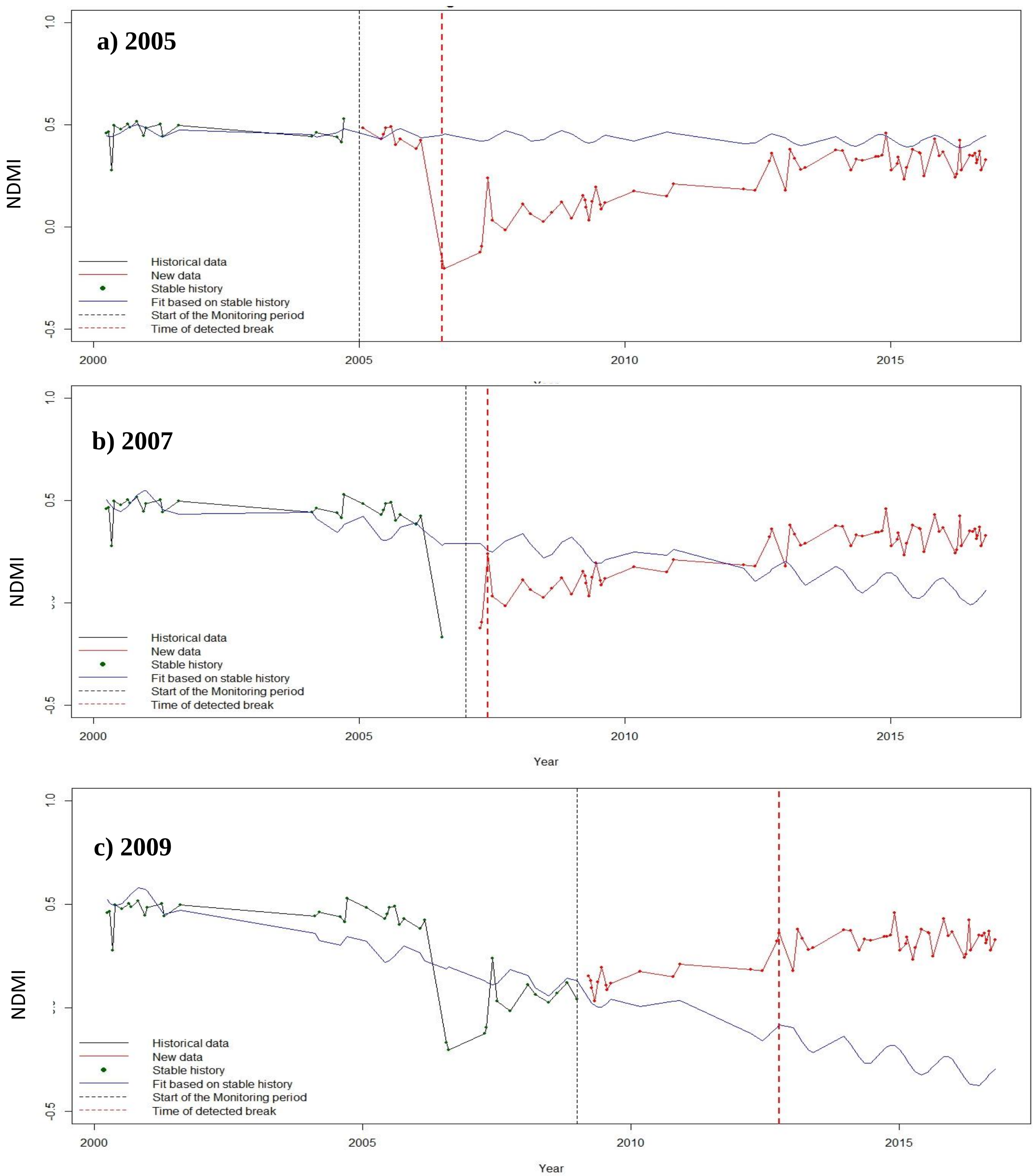

Figure 7: The results of Bfm Pixel, based on the NDMI dataset, with different Start Dates: Julian day 1 of: 2005 (a), 2007 (b) and 2009 (c). The breakpoint (red dashed line) is seen to change drastically in each time-series plot, depending on the timing of the Start Date (black dotted line). The historical data (black line) indicates the "history" period used by Bfast Monitor (BFM) to model the trend and seasonal component. The data points of the "history" period (black dots) are considered as defining a stable history period, by BFM. The breakpoint (red dashed line) is determined by the deviation of the "new data" (red line) from fit of the modelled trend and season (blue line).

3.2.2 Design of change detection method

The first step in detecting spatio-temporal land cover change related to SHOPPs, was to design a method which handles the "Start Date" differently than the original approach. Studies by DeVries et al. (2015a, 2015b) supports the use of a one-year limited monitoring-period, combined with the original premise and input parameters of Bfast Monitor. Furthermore, in this study it has been observed that in some cases, a one-year limited monitoring-period can reduce the risk of detecting false breakpoints during stable land cover time periods. False breakpoints can be caused by a wrongly fitted trend in the historical-period, because of e. g. data gaps or outliers.

To avoid a fixed "Start Date", based on expert-knowledge, the use of a one-year monitoring-period was implemented and extended sequentially to the full time-period of the time-series. This was done by iterating through the time-series with the one-year monitoring-period, from here on referenced to as the "monitoring-window", with a 6-month shift between each iteration, which will be described in detail in section 3.2.4.

3.2.3 Identification of and dealing with data gaps

When an annually iterated monitoring-window is applied, the effect of data gaps on the detection of breakpoints by Bfast Monitor can be substantial (Schultz et al., 2016; Verbesselt et al., 2010). In the original Bfast Monitor method, a "Start Date" is set after any occurring data gap, as any issues related to the data gap will arise during the initial parameter setting steps (or the data set may be abandoned for not having enough data points for trend modelling, at the time-period of interest). Consequences of a data gap can be a wrongly fitted model due to placing the "Start Date" in, or immediately after a data gap.

From the histogram of scenes per year in the Landsat time-series (Figure 8), it can be seen that no scenes were available for 2002 and only one scene was available for 2003. Additional information shows that the one scene in 2003 was collected in late December, which makes the majority of 2003 a data gap as well.

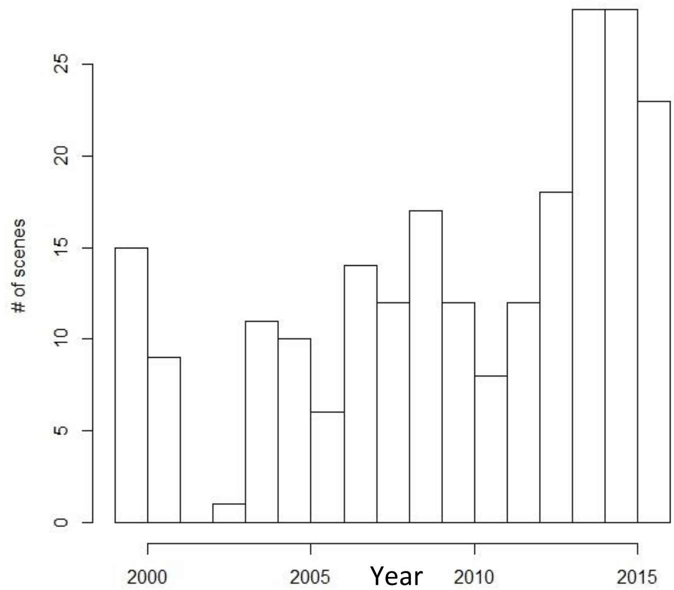

Figure 8: Histogram of the scenes per year for 2000 – 2016, for the NDVI, EVI and NDMI datasets.

A Bfm Pixel test run was performed on a test-pixel from the Land Cover Change class, with the NDMI dataset, to illustrate when the "Start Date" is set within a data gap, here between 2001 and 2004, showed by the green lines (Figure 9). The "Start Date" is set to 2003, Julian day 1, and it is demonstrated how the data gap affects the modelled trend and a false breakpoint is detected in 2004.

When the monitoring window is iterated through the time-series, the "Start Date" will undoubtedly fall within a data gap at some point, if a data gap exists. There is not any control on the quality of intermediate outputs of an iterated procedure, or the opportunity to manually adjust parameters for intermediate functions. Therefore it is recommended that the temporal extent of the input time-series is limited to exclude any identified data gaps, by adjusting the input and output date for the iterated method. The dataset itself is not trimmed, and all data points are therefore still adding information in the breakpoint detection. To diminish the effect of a data gap but still provide enough data for modelling the trend for each iterated monitoring-window, the input and output dates should be set to include a buffer of scenes on each side of the data gap. As seen in the histogram in Figure 8, the data gap spans 2002 and 2003. As a consequence, the time-period analyzed for breakpoints were limited to 2005 – 2016 to avoid the data gap. The previous years, 2000 – 2005, were still included in the historical-period.

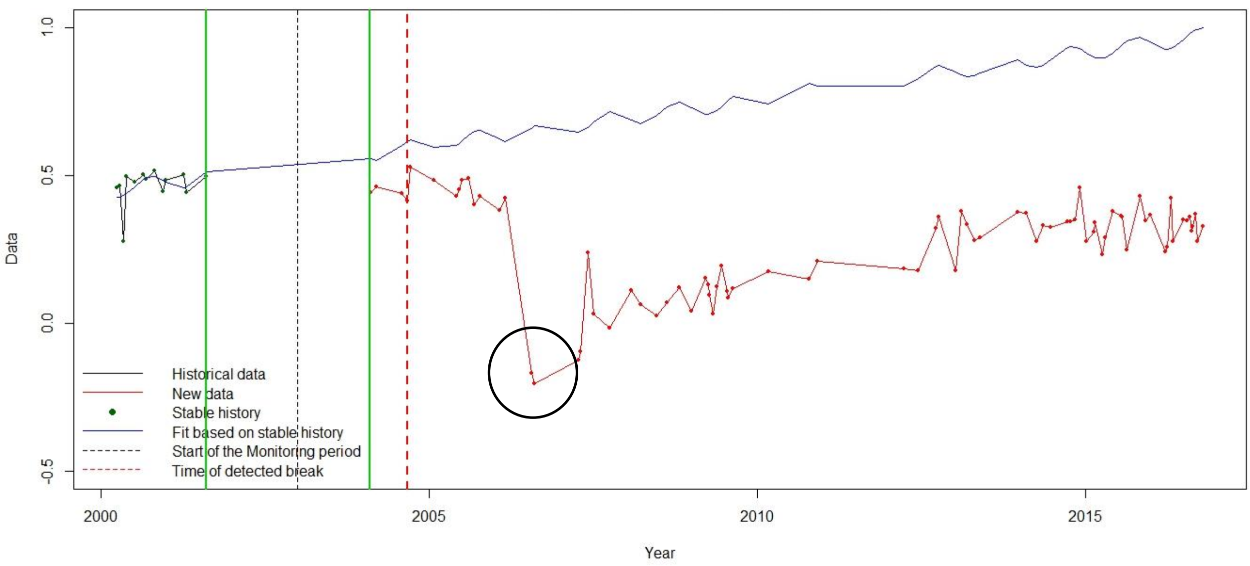

Figure 9: Result of Bfm Pixel, based on the NDMI dataset, illustrating the effect of data gap. The "Start Date" (dotted black line at 2003.1) is set within a data gap, illustrated by the green lines. The modelled trend and season (blue line) is highly affected, and the breakpoint (red dashed line) is not detected where expected, by the drop in the temporal signature (black circle).

The test-pixel shown in Figure 9 was chosen to illustrate the effect of a data gap, however a data gap does not always disrupt the modelling to a degree where false breakpoints are detected.

3.2.4 Implementing the parameters: the annual, six-month shift iteration

The solution proposed in this study to circumvent the conventional use of the "Start Date" parameter is an annual iteration throughout the time-series with a six-month shift. Since the iteration works with a one-year monitoring-window, the end date of the time-series is set to 2015, as 2016 is not a complete year in the dataset (which causes disruptions in the iteration process).

Based on the dataset for Location ID1, 2005-2015, the iteration procedure was structured as shown in Figure 10. The iteration was constructed by defining the "Start Date" and "End Date" parameters, the "End Date" indicating the end of the monitoring-window. The first "Start Date" was set to 2005, Julian day 1 (January 1st, 2005). The "End Date" was set to 2006, Julian day 1 (January 1st, 2006) and outlines the monitoring-window used for the first iteration. This interval is illustrated in figure 10 with the label "1st". The monitoring window was then shifted six months forward and the "Start Date" and "End Date" was thus set to 2005.181 and 2006.181 respectively, illustrated with the "2nd" label in Figure 10. Julian day 181 falls within the final days of June (depending on leap years). The labels of "07-YYYY" are thus chosen to simplify the visualization of the time-line. In every iteration, the end of the historical-period was defined by the "Start Date" and therefore spans from the first date of the dataset (March 1st, 2000) until 2005.1 for the 1st iteration, from March 1st 2000 until 2005.181 for the 2nd and so forth.

The purpose of the six-month shift is to cover the time period immediately after the "Start Date" of the previous iteration. During testing stages of this study, it was observed that visually identified breakpoints right after the "Start Date" are not detected. A reasonable explanation can be that the data point may be considered an outlier by Bfast Monitor (Verbesselt et al., 2012). By implementing a six-month shift, every six months are covered twice and if any breakpoint was missed in the first iteration, it may be detected in the next.

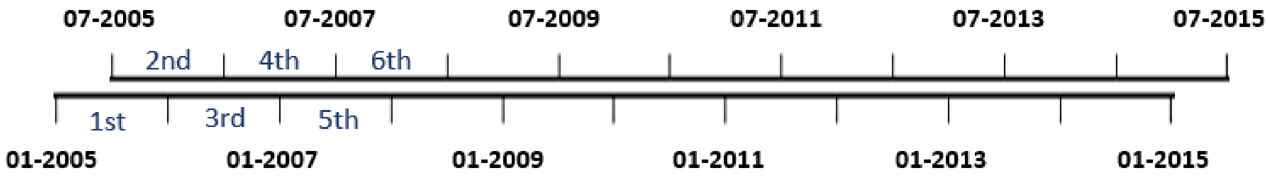

Figure 10: Illustration of the six-month shift. The segmented line above (a) shows one-year time periods from July to July. The segmented line below (b) shows one-year time periods from January to January. The "1st", "2nd", "3rd" etc. labels indicates the order the time-periods are iterated in. First, the time period: 01-2005 to 01-2006 is used. Second, the period: 07-2005 to 07-2006, third: 01-2007 to 01-2008, and so forth.

3.2.5 Selecting the final breakpoint date

The annual, six-month shifted iteration of a dataset covering 11 years has the potential to detect a breakpoint at each iteration, i. e. give 22 results. Since the purpose of the method is to detect one major break, related to one specific breakpoint during the full time series, it is necessary to incorporate a decision rule which can be applied to all the resulting breakpoints. The decision rule should allow for one final breakpoint to remain, which has a higher likelihood of representing the true moment of land cover change in the time-series.

In the original application of Bfast Monitor, it is advised to apply a Magnitude threshold to the output of Bfast Monitor (DeVries et al., 2015a). This suggests that a Magnitude threshold could be applied as a decision rule, since every breakpoint will have a Magnitude value, related to the monitoring-window applied. A Magnitude threshold could be selected the breakpoint that should be included in the final result. This threshold would be determined based on previous knowledge of vegetation dynamics in the area (e. g. it is known that deforestation results in a breakpoint of a certain magnitude) or experimental results.

However, due to the way the Magnitude is calculated (Table 1), some issues can arise from using it as a threshold. During the testing stages of this study, it was observed that breakpoints can be missed to a considerable degree, if outliers or data gaps affects the modelled trend or the dataset. The calculation of the Magnitude is likewise disturbed if high values before the breakpoint exists in the monitoring-period. A similar conclusion was reached by DeVries et al. (2015a) and it is therefore proposed to base the decision rules on the VI value at, or surrounding, the detected breakpoint in the presented approach. Based on the comparison of VI's in section 3.1, the NDMI dataset was concluded as most suitable for the purpose of designing an automated method for land cover change detection related to SHOPPs. The NDMI values was thus used for designing decision rules.

Based on the assumptions regarding the temporal NDMI deforestation pattern, two decision rules were formulated for testing the described approach.

The first decision rule was based on the assumption that the NDMI value at the moment of deforestation (shown as a drop in NDMI values), is relatively low, compared to periods of stable forest. When forest is cleared due to the establishment of oil palm plantations (Verheye, 2010), the NDMI value will drop due to the removal of dense vegetation (Wilson & Sader, 2002). Based on this assumption, a threshold can be set. If the NDMI value of a breakpoint is below this threshold, deforestation is more likely to have taken place as the NDMI value is low enough to represent a clearance of vegetation. To apply the NDMI threshold, Decision Rule # 1 was formulated as follows:

Decision Rule # 1:

- **If** "*the NDMI value of the breakpoint*" **is larger than** "*the selected threshold*", **then** "*the breakpoint*" is **accepted**.
- **If** "*the NDMI value of the breakpoint*" **is less than** "*the selected threshold*", **then** "*the breakpoint*" is **rejected**.

If more breakpoints than one was below the threshold, the earliest dated breakpoint was selected. Based on Decision Rule # 1, one breakpoint value then remained as the final result of the iteration procedure.

In order to produce an experimental output, a conservative NDMI threshold was set to 0.15. This was calculated as the mean between the mean value of the test-pixels of the stable land cover classes and the mean value of the minimum values of each raster in the Landsat raster stack. See Appendix B for the detailed calculation of the threshold.

Based on the same assumptions described in the previous section, the second decision rule was based on the difference between the NDMI values before and after the breakpoint, calculated as ΔNDMI. The assumption was that the mean NDMI value of the period before deforestation (and the detected breakpoint) is relatively high, due to a period of stable forest cover. In the period after deforestation, the mean NDMI values are then relatively low compared to the period before, due to the removal of the forest cover. Calculating the difference between the period before and the period after the breakpoint therefore links a size of the drop associated with deforestation, to the breakpoint. A further assumption was that the maximum ΔNDMI of a time-series (i.e. representing the maximum drop) has the highest likelihood of representing the moment of deforestation. In order to ensure that the ΔNDMI represents deforestation, only positive values are included as detected breakpoints.

To calculate ΔNDMI, the periods before and after the breakpoints are set to one year and the start and end date of each period is defined by a buffer period of three months on each side of the breakpoint. The one-year period is assumed short enough, that no follow-up land cover would affect the temporal signal (DeVries et al., 2015). The one-year and buffer periods are illustrated in Figure 11. Here an example time-series plot is shown to demonstrate the one-year periods and the three-month buffer period.

Figure 11: Illustration of how the ΔNDMI was calculated. When a breakpoint is detected by Bfast Monitor (red line), the data points (dark blue dots) of a one-year period (grey boxes) on each side of the breakpoint, are used to calculate the mean values of the year before and the year after (purple and green lines).

In Figure 11, the one-year period on each side of the breakpoint is shown as the gray areas in the plot. Only data points within these areas are included in the calculation of the mean values. Any data point that falls within the buffer period of six months (white area on each side of the red line) is thus excluded. The calculated means are shown by the purple and the green lines, which also illustrate the data points included in their calculation.

The ΔNDMI is thus calculated as follows:

$$\Delta NDMI = m_{before} - m_{after}$$

with m_{before} = the mean of data points within the year before the breakpoint and m_{after} = the mean of data points within the year after the breakpoint.

The three-month buffer is implemented since the exact structure and characteristics of the data set is unknown during an automated processing sequence. When a breakpoint is detected by Bfast Monitor, it is unknown if there are any data points adjacent to the breakpoint, with NDMI values close to that of the breakpoint. If this is the case, the mean would be highly affected, and not truly represent the period before and after the breakpoint.

To apply ΔNDMI, Decision Rule # 2 was formulated as follows:

Decision Rule # 2

- **If** "*the ΔNDMI of the breakpoint*" **is larger than** "*the ΔNDMI of other reported breakpoints*", **then** "*the breakpoint*" is **accepted**.

- **If** "*the ΔNDMI of the breakpoint*" **is less than** "*the ΔNDMI of other reported breakpoints*", **then** "*the breakpoint*" is **rejected**.

3.2.6 Two methods: *NDMI Threshold* and *ΔNDMI*

The two decision rules were incorporated into two different methods for automatic land cover change detection, both based on the Bfast Monitor pixel-based and raster-based functions: Bfm Pixel and Bfm Spatial. In the following sections, the spatial application of the methods are presented.

Since the spatially applied methods require considerable processing time, it was decided to divide the process up into a separate procedure for each year. This also allows for evaluating intermediate results and gives flexibility regarding the time-frame to process (e. g. if the purpose is to detect land cover change in a particular area, and the land cover change has been detected early on in the time-series, there is no need to process the remaining years).

The raster-based *NDMI Threshold* method was implemented by the following steps:

Input data: Landsat NDMI time-series raster stack, 2000-2016.
Input variables: Start date and end date of monitoring-window.
Experimental threshold: NDMI 0.15

1. The Bfm Spatial function was run for one year at a time, starting with 2005.1.
2. The Bfm Spatial raster output was spatially filtered to remove pixel clusters with an area of less than 1.8 ha (Susila & Bourgeois, 2006). The spatial filter is illustrated in Appendix C.

For every remaining cell where a breakpoint was detected:

3. The corresponding NDMI value of each breakpoint was found.
4. Decision Rule # 1 was implemented:

If NDMI of breakpoint is below threshold, accept breakpoint
If NDMI of breakpoint is above threshold, reject breakpoint

5. The final breakpoint raster for the input year was created: All accepted breakpoints were assigned to their corresponding cell.
6. The spatial filter applied in step 2 was applied to the final breakpoint raster.

Step 1-6 was repeated for every year of the time-series, resulting in 21 breakpoint rasters for the years 2005 – 2015. The final step produces an output map for the full time-series:

7. The 11 annual output rasters were merged with priority to the first occurring breakpoint of a cell.

Similarly to the spatially applied *NDMI Threshold* method, a spatial output of the *⊿NDMI* method is created on an annual basis. The *⊿NDMI* method was implemented by the following steps:

Input data: Landsat NDMI time-series raster stack, 2000-2015.
Input variables: Start date and end date of monitoring-window.

1. The Bfm Spatial function was run for one year at a time, starting with 2005.1.
2. A spatial filter was applied to the Bfm Spatial raster output.

For every remaining cell where a breakpoint was detected:

3. The time-series of each cell is extracted and ΔNDMI of each breakpoint was calculated.
4. A ΔNDMI raster was created by assigning positive ΔNDMI values to their corresponding cell.

Step 1-4 was repeated for every year of the time-series, resulting in 21 breakpoint rasters for the years 2005 – 2015 created by the Bfm Spatial function, and 21 ΔNDMI rasters with the corresponding ΔNDMI values. The following steps were carried out to produce an output raster for the full time-series:

5. The 21 annual breakpoint rasters were merged with priority to the maximum ΔNDMI of a cell.

No threshold was linked to the ΔNDMI value at this point and every breakpoint pixel of the raster (detected by Bfast Monitor) was therefore assigned a value. In order to evaluate the likelihood that a land cover change occurred at the predicted breakpoints, a measure of probability was linked to the magnitude of the ΔNDMI. This leads to Research Question 3: *Can the probability of land cover change be mapped for areas identified as potential change areas?,* and the steps are described in section 3.3.

3.2.7 Validation of the methods

Validation of both methods (*NDMI Threshold* and *⊿NDMI*) was performed with a pixel-based application of each method. Bfm Spatial and Bfm Pixel (which forms the foundation of the pixel-based and the spatial application, respectively) employs the same algorithm, either for each pixel of a raster (Bfm Spatial) or for one target pixel (Bfm Pixel). The algorithm applied per pixel is therefore the same in both functions. The pixel-based version was therefore used, for each method, to validate both pixel-based and spatial outputs.

Confusion matrices were constructed based on a reference dataset and a predicted dataset to determine the accuracy of the methods. The number of sample points were chosen by using the formula for stratified random sampling by Cochran, (1977) with finite population correction applied. The calculation resulted in 758 sampling points, however to allow for points to be omitted (e. g. due to cloud cover), the final sample size was set to 1000.

The reference dataset was created by assigning a "Change" or "No Change" label to each point, determined by visual inspection of high resolution Google Earth imagery, based on the time period: 2006-2014. The pixel-based applications of the *NDMI Threshold* and *⊿NDMI* methods were applied to the 1000 sample points to create the predicted dataset.

Two confusion matrices were constructed for each method. One from the full datasets and one from limiting the datasets to all points visually determined as dense vegetation in 2006 and dense vegetation or oil palm in 2014. This was done in order to limit the datasets to only include points covering the following two classes:

- Dense Vegetation → Dense Vegetation (no change)
- Dense Vegetation → Oil Palm (change)

This limitation was included to describe the accuracy of the methods in detecting specifically deforestation due to SHOPP establishment.

3.3 Mapping the probability of land cover change

Research question 3: *Can the probability of land cover change be mapped for areas identified as potential change areas?* was answered by linking a measure of probability to the output maps created with the spatially applied *⊿NDMI* method for Location ID1. The probability of land cover change was defined as the probability that the predicted breakpoints corresponds to actual land cover change.

In order to map the probability of the detected land cover changes, the following steps were taken:

1. The full reference and predicted datasets created in the previous step (section 3.2.7) were limited to the points labelled "Change" in the reference dataset. This was done in order to calculate the probability that the predicted breakpoints corresponds to actual land cover change.

2. The *⊿NDMI* predicted dataset was divided into categories based on the ΔNDMI value of each point. The categories were defined as "**more than** or **equal to**" values as follows: Category 0: ΔNDMI = 0.00, category 1: ΔNDMI = 0.01, category 2: ΔNDMI= 0.02, category 3: ΔNDMI = 0.03 and so on.

3. Within each category, the probability was quantified with the following calculation:

$$P = \frac{N_{Predict}}{N_{Reference}} * 100$$

Where P = probability, %, $N_{Predict}$ = Number of predicted change points that were actual change, and $N_{Reference}$ = Number of actual change points.

4. A final probability map was made by assigning each breakpoint cell found by the raster-based *⊿NDMI* method, the probability value corresponding to the ΔNDMI value of the cell.

4 Results

4.1 Comparison of NDVI, EVI and NDMI

For the visual comparison of the VI's, time-series plots based on three random test-pixels of the three land cover classes (Table 2) were plotted to observe the temporal profiles of each VI. The result was a total of 27 time-series plots. The temporal profiles revealed that the moment of forest clearance was visually detectable in the majority of the time-series plots. The moment of land cover change was mostly characterized by an abrupt drop in values with a subsequent steady increase (e. g. Figure 12, A). However, the EVI time-series showed a higher frequency of outliers, compared to the NDVI and NDMI time-series (e.g. Figure 12, B).

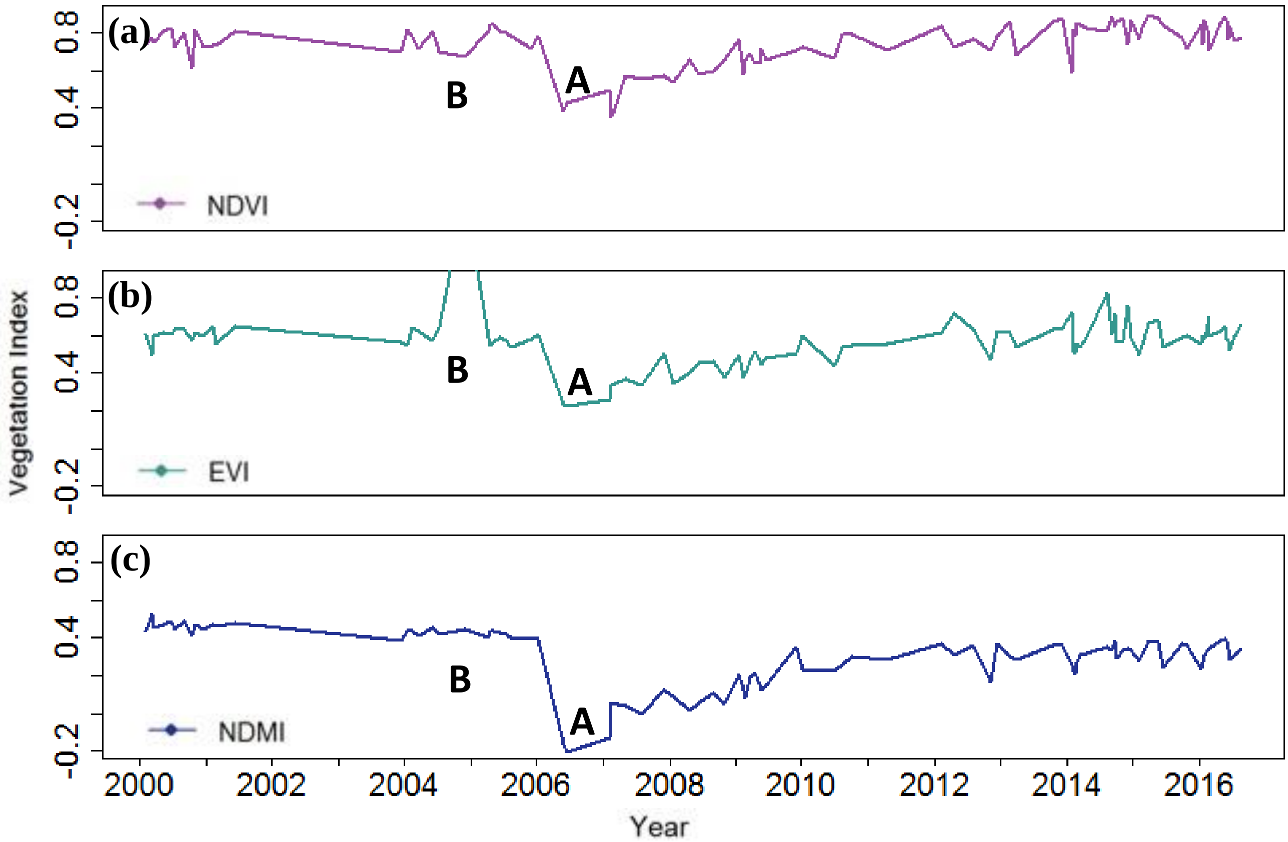

Figure 12: Time-series plots of a random pixel of the Land Cover Change test-pixels (defined in section 3.1.1), based on (a) NDVI, (b) EVI and (c) NDMI from 2000 – 2016 for the same location. Label A represents representing the moment of land cover change and B represents the presence of outliers in the datasets.

For the stable dense vegetation and stable oil palm classes, the EVI temporal profile also showed more outliers than the other two VI's. Between NDVI and NDMI, the NDVI series showed a higher frequency of outliers (Figure 13). The occurrence of outliers in the NDVI and EVI time-series was more frequent during later years of the time-series, likely a result of a higher frequency of Landsat scenes from 2014 and onwards.

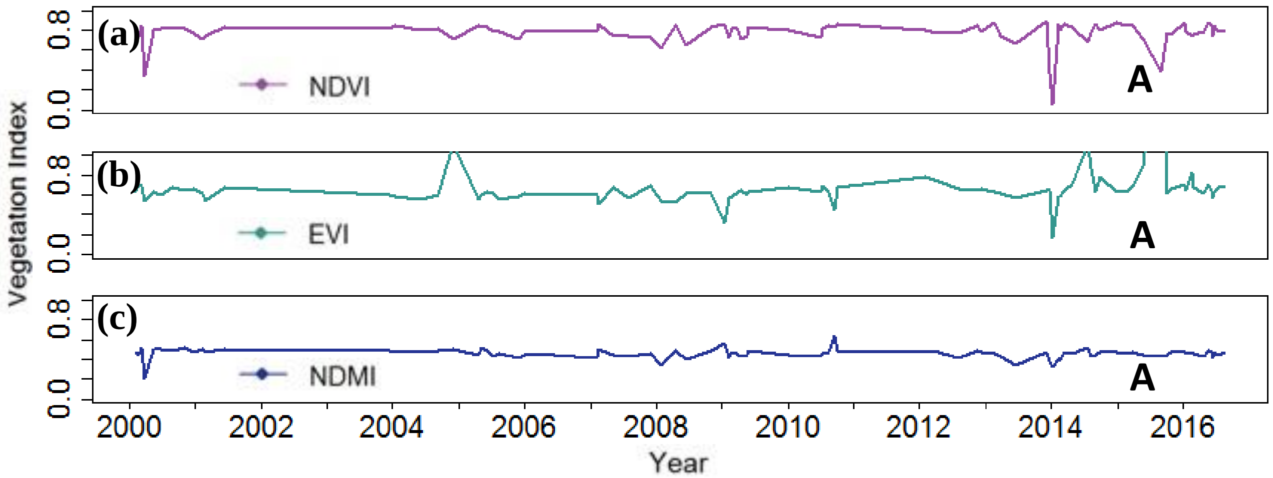

Figure 13: Time-series plots of a random pixel of the Stable Dense Vegetation test-pixels (defined in section 3.1.1), based on (a) NDVI, (b) EVI and (c) NDMI from 2000 – 2016 for the same location. Label A shows a period of time where a higher frequency of outliers are observed in the NDVI and EVI profiles compared to the NDMI profile.

Table 3 reports the results of the visual comparison of the 27 time-series plot based on the three VI's. In this table, the VIs were used to answer the suitability questions defined in section 3.1.2, for the three land cover classes. The VI which received the highest number of "YES" answers in response to the suitability questions were determined to be the more suitable VI for further analysis. The results show that the NDMI received the highest number of "YES" answers, with 14 out of 18 possible, compared to the other VI's, indicating that it is the more suitable index according to the criteria.

Table 3: Comparison of vegetation indices by suitability questions. The first three test-pixels of the three land cover classes were given an answer YES (green) or NO (grey) for each suitability question (Q1 and Q2). For each land cover class, two answers were given for test-pixel 1, test-pixel 2 and test-pixel 3. Q1: Suitability question 1a and 1b: Can a land cover change signature be identified in the temporal signal of the VI, within the Land Cover Change class? Can a stable land cover signature be identified in the temporal signal of the VI, within the stable land cover classes? Q2: Suitability question 2: Can the temporal signal of stable land cover or land cover change easily be recognized without interference from outliers?

YES = NO =

	NDVI			**EVI**			**NDMI**		
	Land Cover Change	Stable Oil Palm	Stable Dense Vegetation	Land Cover Change	Stable Oil Palm	Stable Dense Vegetation	Land Cover Change	Stable Oil Palm	Stable Dense Vegetation
	Test-pixel 1			Test-pixel 1			Test-pixel 1		
Q1	YES	YES	YES	YES	NO	NO	YES	YES	YES
Q2	YES	NO	NO	NO	NO	NO	YES	YES	NO
	Test-pixel 2			Test-pixel 2			Test-pixel 2		
Q1	NO	NO	YES	YES	NO	NO	YES	YES	YES
Q2	NO	NO	NO	NO	NO	NO	YES	NO	YES
	Test-pixel 3			Test-pixel 3			Test-pixel 3		
Q1	YES	YES	YES	YES	NO	NO	YES	YES	YES
Q2	NO	NO	NO	NO	NO	NO	NO	NO	YES

The results of the comparison of the NDVI, EVI and NDMI, based on Bfm Pixel test runs of the 100 test-pixels are presented in Table 4. The results are shown as the number of false breakpoints detected within each land cover class, based on each VI dataset. The NDVI series gave the highest number of detected false breakpoints for all land cover classes (81) and NDMI the lowest (55). Looking into each land cover class separately, the lowest number of false breakpoints detected in the Stable Oil Palm and Land Cover Change classes were also based on the NDMI. In the Stable Dense Vegetation class, all VIs achieved high numbers of detected false breakpoints. Based on the NDVI, 37 out of 37 points were false breakpoints, based on the EVI and NDMI, 31 and 35 out of 37 were falsely detected breakpoints, respectively. All VIs detected false breakpoints in the Land Cover Change class, which is a results of breakpoints being detected at other dates than expected, from visual evaluation of the temporal profiles of each test-pixel.

The amount of false breakpoints is likely a result of not adjusting the parameters of Bfm Pixel for each point individually (the parameters were adjusted for each VI, not each point). Furthermore, no Magnitude threshold was applied, which would likely also reduce the numbers of false detected breakpoints in the stable land cover classes. These conditions were the same for all VI's and the results are therefore appropriate for a comparative analysis, however they do not reflect the optimized performance of the Bfast Monitor algorithm (DeVries et al., 2015).

With the lowest number of false breakpoints detected in total and for two out of three land cover classes, based on the NDMI dataset, the NDMI was the better performing vegetation index for land cover change detection with the Bfast-algorithm.

Table 4: Comparison of the NDVI, EVI and NDMI datasets based on the number of false breakpoints detected in each land cover class by Bfm Pixel. The dark blue boxes indicates the highest number of false breakpoints detected, the medium blue indicates the intermediate number and the light blue indicates the lowest number.

Land Cover Class	Number of samples	**NDVI** -based false breakpoints	**EVI**-based false breakpoints	**NDMI**-based false breakpoints
Stable Dense Vegetation	37	37	31	35
Stable Oil Palm	29	28	15	14
Land Cover Change	34	16	24	6
Total	***100***	***81***	***70***	***55***

The NDMI had the best performance in the visual comparison and detected the lowest number of false breakpoints in the Bfm Pixel test-runs, compared with the EVI, NDVI and NDMI datasets. The NDMI was therefore selected as the most suitable VI for detecting the conversion of forest to oil palm plantation and used for further analysis in this study.

4.2 Comparison of methods for spatio-temporal detection of land cover change

4.2.1 The pixel-based *NDMI Threshold* and *ΔNDMI* methods

The results of running the methods on the 100 test-pixels defined in section 3.1 1, are presented in Figure 14a and b. For each point the year of change was assigned, as detected by the pixel-based *NDMI Threshold* method (Figure 14a) or the *ΔNDMI* method (Figure 14b) or "No Breakpoint" if no change was detected.

The result of pixel-based *NDMI Threshold* method with the experimental threshold of 0.15, shows that breakpoints were only detected within the Land Cover Change area, where each point was assigned a year of change (Figure 14a). The breakpoints were detected in 2006, 2008, 2009 and 2010, and are grouped by their detected change year, indicating a possible deforestation pattern of the area.

The *ΔNDMI* method resulted in detected breakpoints in 2005 – 2010, 2014 and 2016, detected in the Land Cover Change area and the Stable Dense Vegetation area (Figure 14b). In the Land Cover Change area, the detected change points are distributed similarly to the result in Figure 14a, except with a few points detected in 2007. Since the 2007 points are located between breakpoints detected in 2010, the 2007 points does not appear likely to be a part of a deforestation pattern. The breakpoints detected in the Stable Dense Vegetation class does not appear to represent any pattern of change as they are not grouped by their year of change.

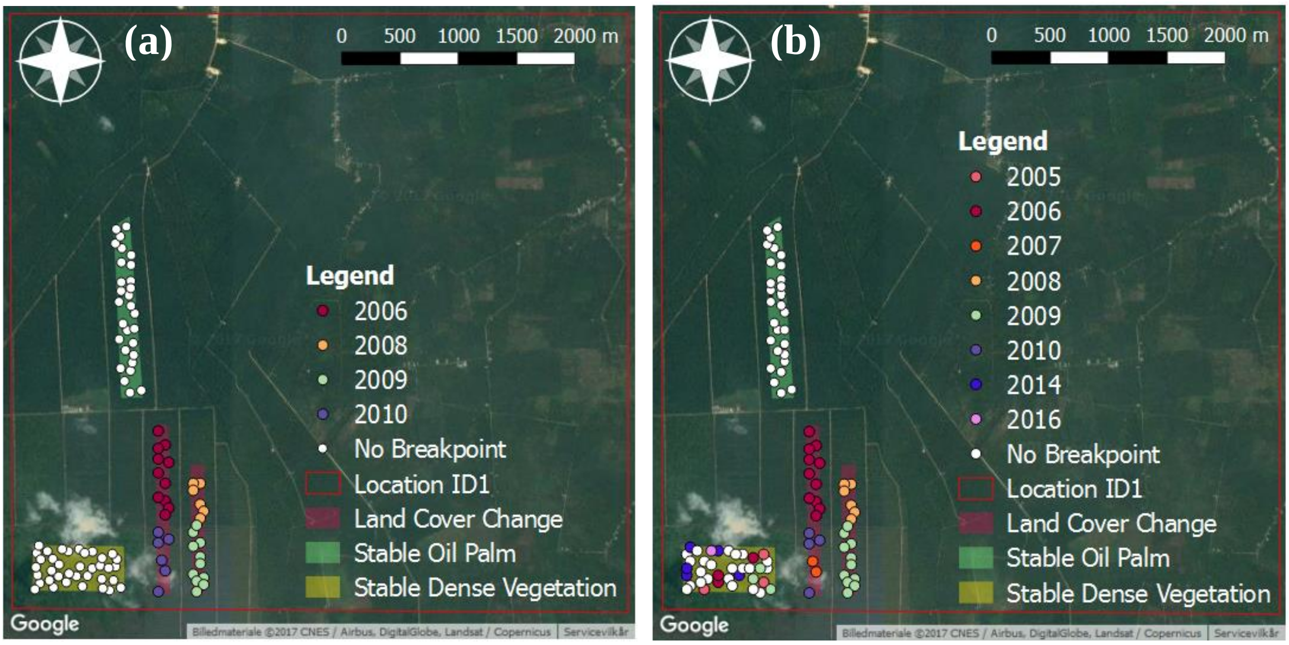

Figure 14: Results of the pixel-based NDMI Threshold method (a) and the pixel-based ΔNDMI method (b). The methods were run on the 100 test-points, and the color of the points indicate the year of land cover change detected by the methods.

By comparing the results of the two methods (Figure 14a and b), the main difference is seen in the number of detected breakpoints in the Stable Dense Vegetation class. The *NDMI Threshold* method did not detect any breakpoints in this class, while the *ΔNDMI* method detected 15 breakpoints out of the 37 points. This is likely a consequence of not applying any threshold in the *ΔNDMI* method. The NDMI-based Bfm Pixel runs on the same test-pixels, presented in the previous section, resulted in 35 breakpoints out of the 37 "stable" points. The number of breakpoints detected in the Stable Dense Vegetation class were decreased considerably by applying the *⊿NDMI* method, and no breakpoints were detected by applying the *NDMI Threshold* method.

4.2.2 The spatial application of *NDMI Threshold* and *ΔNDMI* methods

The result of the spatial application of *NDMI Threshold* method (Figure 15a) for the time-series of 2005 – 2015, was achieved with the experimental threshold of 0.15. Land cover change in Location ID1 was detected for approx. 16% of the total area, for the years 2005 – 2011 and in year 2013 and 2014. Rectangular and systematic patterns of land cover change were detected in the South-West corner (label A, Figure 15a), while scattered patches of land cover change, were found in the North-East part of Location ID1 (label B, Figure 15a).

The raster-based *⊿NDMI* method detected land cover change for approx. 24% of the area, in every year from 2005 – 2015 (Figure 15b). A similar rectangular pattern of land cover change is found in the South-West part of Location ID1 (label A, Figure 15b). In the North-East corner, a higher amount of land cover changed patches were detected (label B, Figure 15b), compared to Figure 15a.

The main difference between the two results is the total size of land cover change areas detected, where the area detected by the *⊿NDMI* method was approx. 24% of the total area, the *NDMI Threshold* method detected land cover change for approx. 16%. Both results are considerably smaller than the total area detected by the original output of Bfm Spatial (Figure 15c) of approx. 48%. The larger change area observed in figure 15c is resulted from not applying a spatial filter or threshold to the breakpoints detected by Bfm Spatial. Furthermore, the output was not limited to breakpoints caused by deforestation.

By comparing the resulted maps of the two methods visually, a high similarity in the location and timing of detected land cover changes is observed. Both methods were designed to detect land cover change due to deforestation, and it is therefore likely that the areas detected as change by both methods (e. g. by label A, Figure 15a and b were caused by removing forests or other types of dense vegetation. In Figure 15b by label B, patches of change pixels are observed which are absent in figure 15a. A pattern also seen in the output of Bfm Spatial (Figure 15c, label B), however with a higher pixel density in the area.

These results show that the threshold applied in the *NDMI Threshold* method, highly limits the size of the area detected as change, compared to the Bfm Spatial output. This further supports the likelihood that only a certain type of land cover change (deforestation) was detected by this method. The result of the *⊿NDMI* method is also limited, but to a lesser degree. The result was limited by only including breakpoints with a ΔNDMI value above zero. By incorporating a threshold based on the ΔNDMI values of the breakpoints, the area detected would likely be increased further.

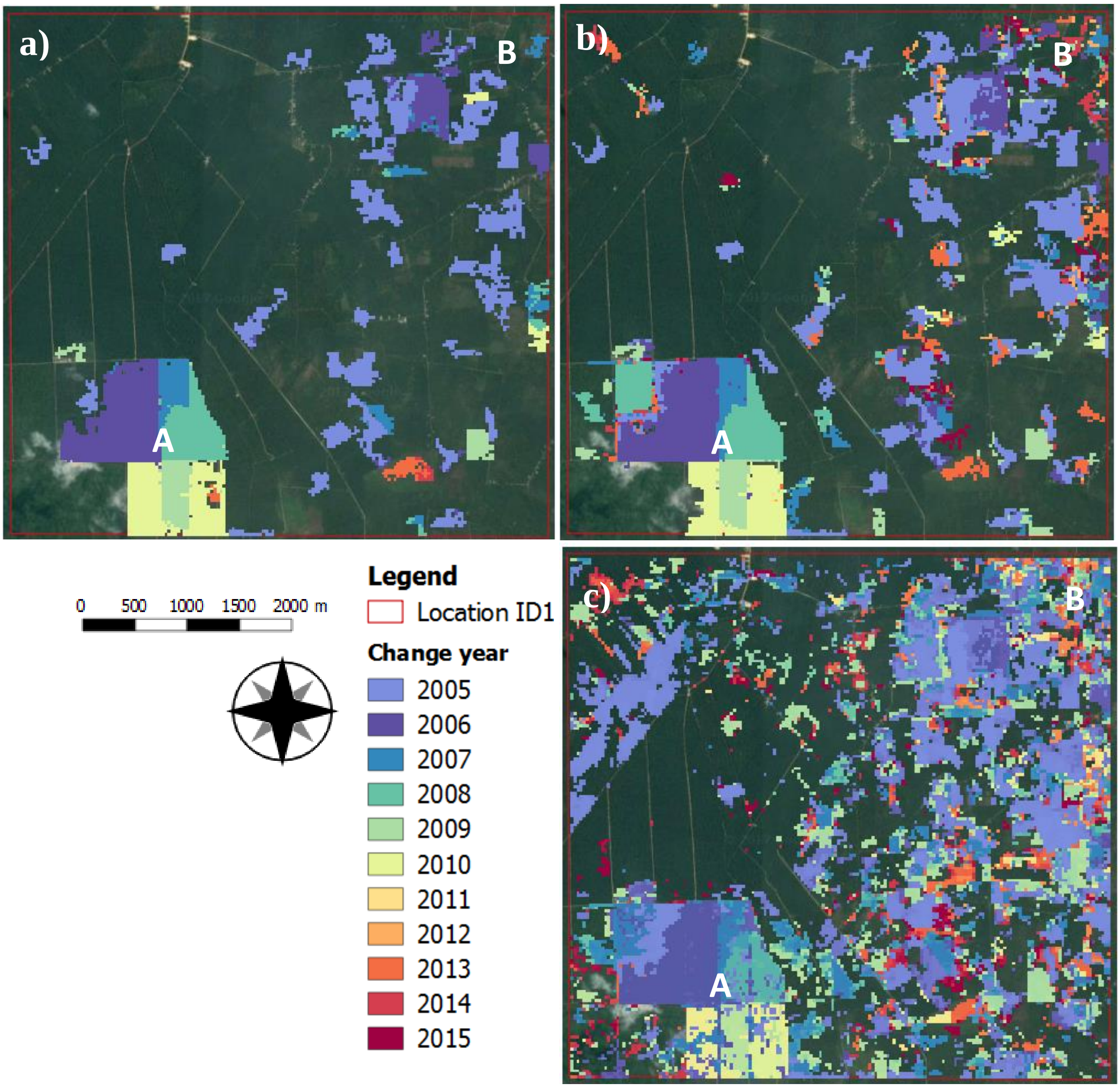

Figure 15: The timing and location of land cover change detected for 2005 – 2015. a): the NDMI Threshold method, (b): the ΔNDMI method, c): The output of Bfm Spatial. Land cover change was detected in rectangular, coherent patterns (A) and in irregular, scattered patches (B).

4.2.3 Validation of the *NDMI Threshold* and the *ΔNDMI* methods

Validation of both methods was performed by applying the pixel-based versions of each method to 1000 random sample points within Location ID1, as described in section 3.2.7. Since both the pixel-based and spatial application of the methods detect land cover change by implementing the Bfast-algorithm per pixel, the pixel-based versions serve as validation for the spatial application as well.

The reference dataset were cleaned from points where a "Change" or "No Change" label could not be assigned (e.g. due to cloud cover or uncertain visual evaluation). Secondly, points with change detected before or after 2006 – 2013 were excluded from both the reference and predicted datasets, since these could not be validated by Google Earth imagery. Since the number of change pixels detected before or after 2013 were different for each method, the final number of reference points used for validation was different. For *NDMI Threshold*, 893 points remained, and for *ΔNDMI*, 767 remained. The distribution of points were approx. 62.5% and 64.5% belonging to the "No Change" class, for *NDMI Threshold* and *ΔNDMI*, respectively.

The accuracies achieved based on the full reference dataset were 74.6 % and 76.3 % for the *NDMI Threshold* and the *ΔNDMI* methods, respectively (Table 5), for changes that occurred in 2006 – 2014.

Table 5: The overall, Producer's and User's accuracies achieved by the NDMI Threshold and the ΔNDMI methods, including all types of land cover change, in year 2006 – 2014.

	Overall (%)	Producer's Accuracy (%)		User's Accuracy (%)	
	All land cover types	**Change**	**No Change**	**Change**	**No Change**
NDMI Threshold	74.6	34.9	98.4	92.9	71.6
ΔNDMI	76.3	55.2	89.7	73.4	77.5

Looking into the classes separately, the *NDMI Threshold* achieved the lowest accuracy of all, of 34.9% of the actual change points that were correctly predicted as change (Producer's accuracy, i.e. correctly detecting actual change), and the highest accuracy of all in correctly detecting no change (98.4% in Producer's accuracy). The *NDMI Threshold* method thus detected no change with a considerable higher accuracy than change was detected. In User's accuracy however, *NDMI Threshold* could achieve an accuracy of 92.9% in number of predicted change that were actual change. So even though only approx. one third (34.9%) of the actual change points were correctly detected, the majority (92.9%) of all predicted change points were correct.

The *ΔNDMI* method similarly achieved its highest accuracy in actual change points that were correctly predicted as no change (89.7%, Producer's accuracy), and its lowest accuracy in actual change points that were correctly predicted as change (55.2%, Producer's accuracy).

Table 6: The overall, Producer's and User's accuracies achieved by the NDMI Threshold and the ΔNDMI methods, for land cover change related to dense vegetation, in year 2006 – 2014. "Change": dense vegetation changed into oil palm. "No Change": dense vegetation that remained dense vegetation.

	Overall (%)	Producers Accuracy (%)		Users Accuracy (%)	
	Dense Vegetation	**Change**	**No Change**	**Change**	**No Change**
NDMI Threshold	92.4	92.5	92.1	96.1	85.4
ΔNDMI	88.3	97.4	66.7	87.4	91.7

The accuracies achieved from limiting the datasets to only include: dense vegetation → dense vegetation ("No Change") and dense vegetation → oil palm ("Change"), were 92.4% and 88.3% for the *NDMI Threshold* and the *ΔNDMI*, respectively (Table 6). The obtained accuracies are again similar for both methods. Looking into the classes, *ΔNDMI* achieved the highest accuracy of all, with 97.4% of actual change points that were correctly predicted as change (Producer's accuracy), while the largest accuracy achieved by the *NDMI Threshold* method in number of predicted change that were actual change (96.1%, User's accuracy). The *ΔNDMI* method achieved the lowest accuracy in actual change points that were correctly predicted as no change (66.7% in Producer's accuracy) and the lowest accuracy for the *NDMI Threshold*, were in in number of predicted no change that were actual no change (85.4%, User's accuracy).

From the results of the accuracy assessments, it can be concluded that similar accuracies were achieved by both methods. The accuracies were obtained without using the previously defined expert-knowledge, required by the original Bfast Monitor method, and both historical and near real-time detection of land cover change was accomplished.

4.3 Probability mapping

The probability of how accurately the *ΔNDMI* method can correctly detect land cover change, was calculated for the ΔNDMI categories: ΔNDMI 0.00 – ΔNDMI 0.49 (interval: 0.01) (Figure 16). The ΔNDMI categories were defined as "**more than** or **equal to**" values, so the ΔNDMI 0.00 category includes all ΔNDMI values **more than** or **equal to** 0.00, and so on.

From the results, the lowest probability is found for category 0.00 at approx. 73% (Figure 16). Since the ΔNDMI 0.00 category includes all positive ΔNDMI values and therefore all breakpoints detected by the *ΔNDMI* method, the probability of any land cover change detected by the *ΔNDMI* being actual change, is 73%. If a threshold was applied to the ΔNDMI values of the detected breakpoints, the probability of the method detecting change accurately, would increase according to the graph shown in Figure 16. For all ΔNDMI categories above 0.22 (red point, Figure 16), a probability of 100 % was reached. A threshold of ΔNDMI 0.22 would thus result in 100% probability of the land cover change detected by the *ΔNDMI* method is true change, according to the reference dataset.

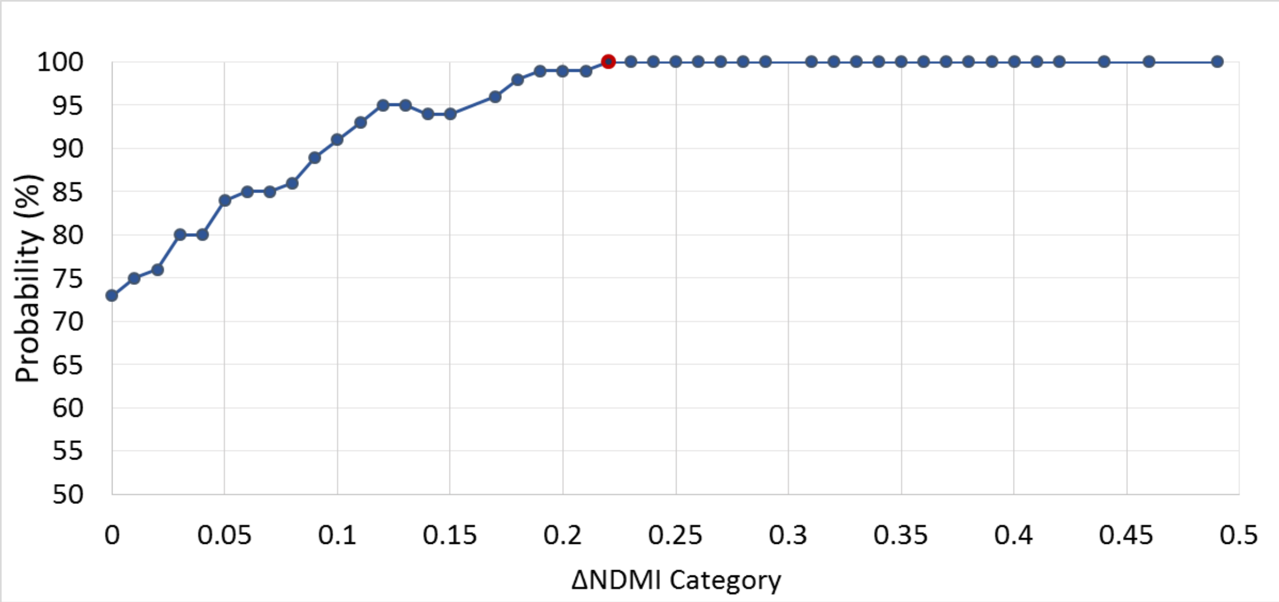

Figure 16: The probability of accurate detection of land cover change for each ΔNDMI category. The ΔNDMI categories are defined with a 0.01 interval. Gaps in the blue plot, e. g. at ΔNDMI category 0.45 are a consequence of no points having a ΔNDMI value of 0.45. The red point illustrates that a probability of 100% is reached at ΔNDMI category 0.22.

A probability map was created based on the probabilities assigned to each ΔNDMI category. The probability areas are shown in Figure 17 and correspond to the detected land cover change areas in Figure 15b. Compared with the corresponding change years (Figure 15b), it is notable that the areas of lower probability mostly relates to recent change years, after year 2010, e. g. the low probability patch by label A, Figure 17, which was detected in 2015 (Figure 15b). Furthermore, from Figure 17 it can be seen that the majority of low probability areas are smaller patches (label B) while larger patches (label C and D) generally have a higher probability of being correctly detected land cover change.

The relatively low probability is a result of a low ΔNDMI value (approximating zero) of the detected breakpoint, a consequence of a similar mean NDMI value in the year before the breakpoint, to the mean value the year after. This can indicate that another type of land cover change occurred than deforestation, or that false breakpoints were detected. Outliers in the dataset could likewise result in unexpected ΔNDMI values, however this option is less likely since a pattern could be recognized for the breakpoints with lower probabilities. Other notable facts are that the low probability areas were detected in years and in locations mainly absent in Figure 15a. Thus, the breakpoints of the areas did not occur at NDMI values below 0.15, the selected threshold for detecting deforestation with the *NDMI Threshold* method.

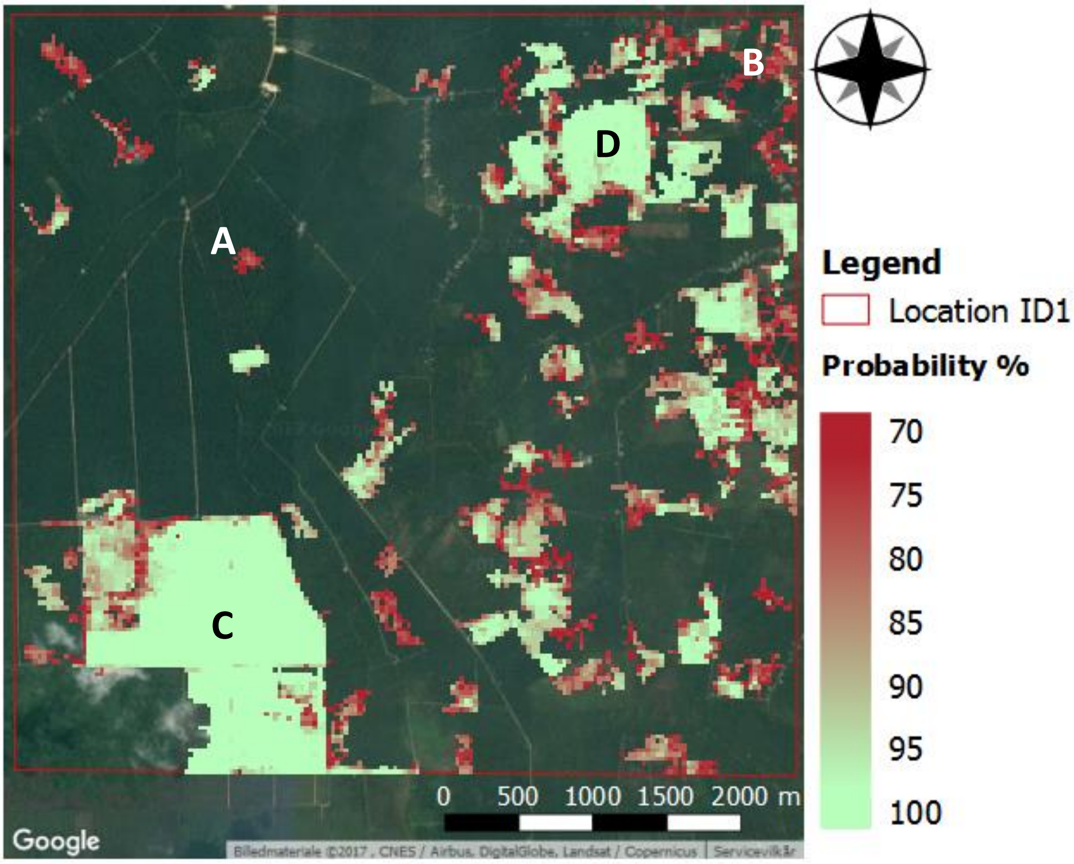

Figure 17: The mapped probabilities of the land cover change detected by the ΔNDMI method. Label A: example of a low probability patch detected in recent years, according to figure 13 (b). Label B: Example of relatively smaller, scattered low probability patches. Label C and D: Example of a relatively larger, high probability patch.

5 Discussion

In this study, Bfast Monitor was integrated into an automated approach, with the purpose of detecting deforestation caused by Smallholder Oil Palm Plantation (SHOPP) establishment.

The results showed that NDMI was more suitable vegetation, for detecting land cover change with the Bfast-algorithm, as compared to NDVI and EVI. Furthermore, two distinct methods for detecting spatio-temporal land cover change were presented: the *NDMI Threshold* and the *⊿NDMI* method. Both methods obtained similar accuracies, but are characterized by different advantages and disadvantages. Finally, a probability of the *⊿NDMI* method correctly detecting land cover changes, was mapped. These results will be discussed in the following sections.

5.1 Choice of vegetation index for time-series analysis with Bfast Monitor

The choice of NDMI as the foundation of this study, was made based on visual interpretation of time-series plots and Bfm Pixel test-runs. Previous studies using the Bfast-algorithm were mostly based on NDVI datasets, either derived from MODIS or Landsat imagery (e. g. DeVries et al., 2015a; Schultz et al., 2016; Verbesselt et al., 2010, 2012), except the study by Dutrieux et al. (2016) and DeVries et al. (2015b). Dutrieux et al. (2016) successfully used NDMI to reconstruct land use history in Brazil, whereas DeVries et al. (2015b) monitored disturbance and regrowth of tropical forests in Peru. Based on experience from ISCC/GRAS (GRAS - Global Risk Assesment Services, 2015), it was decided to compare different vegetation indices for this study.

Since both comparison methods were highly influenced by outliers and noise, the strength of the temporal signals of each VI, could likely have been improved by temporal filtering. Several filters exist, however temporal filtering was usually not employed for studies using Bfast Monitor (e.g. Dutrieux et al., 2016), since the algorithm is not considered sensitive to outliers (Verbesselt et al., 2012). However, a considerable amount of false breakpoints were still detected by Bfast Monitor, based on all three VIs (Table 4). If the datasets had been temporally filtered, this amount would likely have decreased, and thus the suitability of the NDVI and EVI could likewise have been increased. However, the premise was the same for all VI's and the NDMI could still be concluded suitable without temporal filtering of the datasets, limiting the necessary pre-processing steps.

The choice of NDMI in general, carries some limitations that needs to be considered. The NDMI is a moisture index, which is sensitive to the moisture contained in land covers, e. g. the moisture content of soil and foliage (McDonald et al., 1998; Thenkabail, 2016). Limitations therefore exists in extrapolating the land cover change detection methods presented in this study, to different geographic regions. The *NDMI Threshold* and *⊿NDMI* were designed specifically for the purpose of detecting deforestation related to oil palm plantations, which are cultivated in humid tropical lowlands (Verheye, 2010). The climate of the study area, the Riau Province, Indonesia, is characterized by a dry and wet season, with high humidity throughout the year and an annual rainfall of 2500 to 3000 mm (Biagioni et al., 2015; Motohka et al., 2014). Seasonality is present, defined by the dry and wet season, however the wet season usually spans 9-10 months (September-May), and the minimum rainfall observed in June is approx. 100-150 mm (monthly mean, Biagioni et al., 2015). Since seasonality was observed in time-series based on both NDVI and EVI in previous studies related to oil palm, (Gutiérrez-Vélez & DeFries, 2013; Panuju & Trisasongko, 2012), the humid tropical climate likely caused the little seasonality observed in the NDMI time-series (e.g. Figure 12 and 13), due to NDMI's sensitivity to moisture. Since the variables (i.e. NDMI threshold and ΔNDMI) defined in this study, were designed based on the characteristics of the NDMI time-series, the automated methods are therefore highly advantageous for application in humid, tropical regions. It is therefore also likely that they can prove disadvantageous for application in climate regions, experiencing a higher degree of seasonality, compared to South-East Asia. However, previous studies based on Landsat-derived NDMI time-series for forest disturbance detection (Hais et al., 2009; Jin & Sader, 2005; Wilson & Sader, 2002) were conducted in continental and temperate climate zones, suggesting that, with modifications, an NDMI based tool can be useful in other climate regions. Further testing in areas of different climate is necessary to verify this potential.

5.2 The *NDMI Threshold* method

The *NDMI Threshold* method was designed as an automated approach (i.e. not applying the needed expert-knowledge) to the Bfast Monitor method, and uses the exact NDMI value of the breakpoint detected by Bfast Monitor, to create a final result.

The main advantage of the *NDMI Threshold* is its independency of noise and outliers that can be present in the time-series. If the NDMI threshold is set to the value providing the highest accuracy, the probability of detecting false breakpoints is expected to be minimal, based on the findings of this study. Previous studies have as well found the implementation of a threshold beneficial in land cover change detection, in order to separate the temporal change signal from seasonal variability, outliers and noise, however based on a number of different approaches (Cai & Liu, 2015; Kennedy, Yang, & Cohen, 2010; Potter et al., 2003; White & Nemani, 2006). Further research is still needed to test the method, and to determine the threshold with the most accurate outcome. An approach could be to apply the *NDMI Threshold* method for a number of test pixels at a range of threshold values (f. ex. between 0.00 - 0.50), and quantify the correctly detected breakpoint for each value, by reference to ground truth data.

The need for a threshold is an obvious disadvantage, as it requires extensive costs and efforts to determine the threshold (Verbesselt et al., 2012), which will result in the most accurate outcome. The NDMI threshold used in this study (i.e. 0.15) is experimental, and adjusting the value would greatly influence the final output of the method. For instance, the size of the detected change area would decrease if a lower threshold was applied (Figure 18).

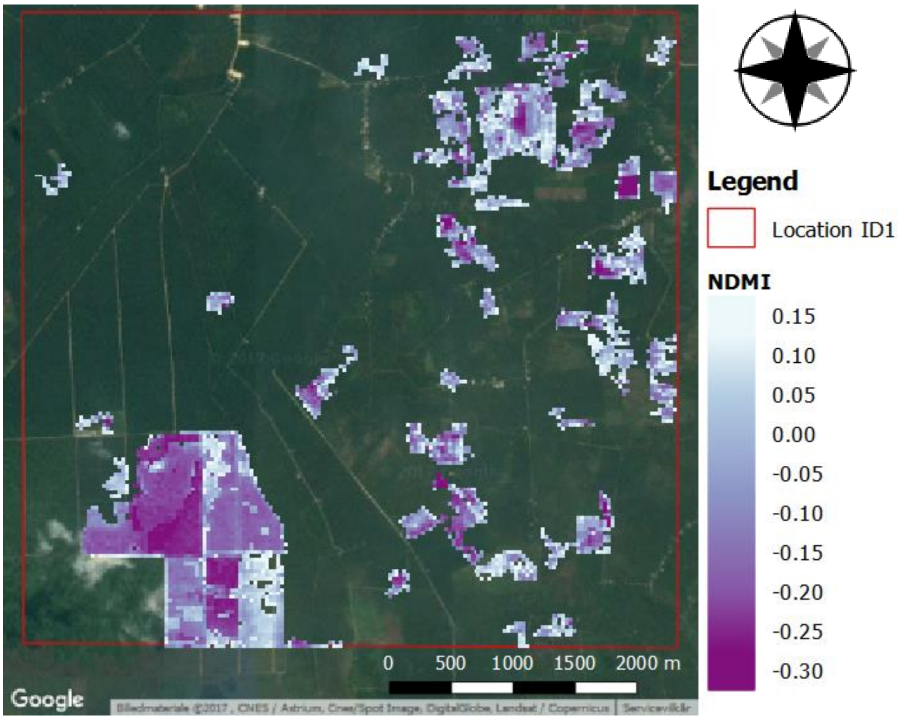

Figure 18: The NDMI values of the breakpoints detected by the NDMI Threshold method from 2005 – 2015. According to the experimental threshold, all NDMI values are below 0.15.

Furthermore, applying the NDMI threshold results in limitations related to the following concepts and components of this study:

- The vegetation index: The method is founded on the Landsat NDMI, and the threshold is an NDMI value, and obviously therefore only applies to an NDMI based time-series. As discussed in the previous section (section 5.1), the method could be successful with other Landsat-derived VI's, and the threshold defined and implemented in this study would thus not apply.

- Type of change: While it can be considered an advantage that the method is flexible regarding the type of land cover change detected (be determining different thresholds for different types), it is likewise a disadvantage that extended research is necessary for determining different thresholds. The threshold was set based on the expected temporal NDMI signal of deforestation (a sudden drop in NDMI value, to a relatively low value at the moment of land cover change). If another type of change occurs, characterized by a different temporal pattern, such grassland → oil palm, the threshold should be adjusted accordingly.

- Geographic location: The NDMI reflects minimal seasonality (as modelled by Bfast Monitor), and the little seasonal variability observed is directly related to the location of the study area in a tropical region. If high seasonal variability was present in the dataset, a vegetation index-threshold could be problematic, since large fluctuations would change the characteristics of the dataset, requiring an entirely different approach.

Because of the aforementioned constraints, the threshold can be optimized to provide a highly accurate result, with the purpose of detecting deforestation (or plantation conversion) due to oil palm plantation establishment in tropical regions. However, flexibility or the possibility of extrapolating the method to other non-tropical geographic regions or other types of land cover change is very likely lost by introducing a threshold of an absolute VI value (White & Nemani, 2006).

The accuracy assessment was conducted with the pixel-based *NDMI Threshold* method for 1000 random points within Location ID1. An overall accuracy of 74.6% was achieved, and looking into the land cover classes individually, the lowest Producer's accuracy (34.9%, Table 5) of the "Change" class was likely caused by the defined threshold 0.15. In the full dataset, no distinction is made between types of land cover change. For example, if grassland was converted to oil palm, the breakpoint would be detected when a change in the time-series occurred, at the point when the NDMI values were increasing compared to the stable grassland condition. The NDMI value of the breakpoint would then be higher than during deforestation, where the breakpoint would occur at the moment of clearing the forest cover. Since the threshold was designed in order to detect deforestation, it is expected that other types of land cover change can be missed by the method.

The high accuracy (98.4%) of the "No Change" class however, shows that the method detected very few false breakpoints. The *NDMI Threshold* method, applying the experimental threshold, can thus be concluded to perform relatively better in correctly detecting "no change", than in detecting the actual timing and location of land cover change (according to the reference, Google Earth imagery). Since the threshold is experimental, further studies could suggest a better performing threshold, as discussed above, and thus improve the overall performance of the method.

To determine the ability of the method to detect land cover change specifically related to deforestation caused by SHOPP establishment, the reference and predicted datasets were limited to only include dense vegetation. Compared with the full dataset in Table 5, a higher accuracy was achieved with the limited dataset (92.4%, Table 6), which suggests that the performance of the method has increased considerably, when only land cover change related to dense vegetation is taken into account. Compared with the performance based on the full datasets, the method is here more likely to detect actual land cover change, with an accuracy of 92.5% (Producer's accuracy in the "Change" class) versus 34.9%. This result supports the conclusion that the performance of the method is relatively better in detecting one type of land cover change (deforestation), compared to other types.

It is concluded that, while the threshold is a disadvantage, it can be optimized to provide a highly accurate result, with the purpose of detecting deforestation due to oil palm plantation establishment in tropical regions.

5.3 The *ΔNDMI* method

The *ΔNDMI* method is the second proposed solution for an automated approach to the Bfast Monitor change detection method. The *ΔNDMI* method uses the difference in the temporal pattern before and after the breakpoint detected by Bfast Monitor, to determine the magnitude of change.

The main advantage is that no threshold is required, which provides flexibility since a specific threshold accustomed to the type of land cover present is needed. A probability measure for determining the probability of the *ΔNDMI* method correctly predicting land cover change, could be linked to the ΔNDMI values, which also provides a tool for setting a threshold based on the found probabilities, e. g by only including areas with a probability higher than 95% (section 4.3).

The definition of ΔNDMI (i.e. the size of a detected change), the concept could in theory be implemented with other VI's. As concluded from visually comparing the VI's, a land cover change signal could be identified in most of the NDVI and EVI time-series plots. While further testing of the method is needed, it is likely that the method can work with other VIs, e.g. EVI which has previously been successfully applied in time-series based change detection related to do oil palm plantations (Gutiérrez-Vélez & DeFries, 2013).

Another advantage of *ΔNDMI* is that it can be further improved to characterize the different types of changes recorded, e. g. by including breakpoints with negative ΔNDMI values, which would indicate growth of dense vegetation. This requires further research into how the ΔNDMI values can be representative of different types of change, still the *ΔNDMI* method has the potential to be a method, which does not depend on a threshold, and is capable of detecting the both the location, timing and type of land cover change.

The main disadvantage of the method is the calculation of the ΔNDMI. Since ΔNDMI relies solely on the dataset, and thereby the temporal distribution and density of data points in the time-series, calculating the value becomes highly sensitive to the characteristics of the dataset. If noise, outliers and data gaps affects the temporal signal of the two one-year periods used to calculate the ΔNDMI, the value will be distorted accordingly. A precaution was built into the method, by returning no value if a data gap does not allow for calculating a mean in any of the periods, and no output is returned, even though Bfast Monitor were able to give a result. A solution for the problem of data gaps could be to locate the nearest stable period on each side of the breakpoint in the dataset. Some criteria could be defined: the number of data point values should fall within a specific period of time to represent a stable period. The mean of these could then be used to calculate the ΔNDMI. The defined three-month buffer and one-year before and after periods could likewise be re-defined by a similar criteria.

If outliers disturb the value of ΔNDMI, the output can likely be improved by applying a temporal filter to increase the quality of the dataset (Chen et al., 2004), as discussed previously. Similar to the limitation of *NDMI Threshold* method, the characteristics of the temporal signal is key to the concept of the *ΔNDMI* method. While this method is more flexible by not including a threshold, limitations remain in extrapolating the method to non-tropical regions. Fluctuations caused by seasonal variability in the temporal pattern belonging to non-tropical vegetation, e.g. boreal, would create difficulties in calculating a meaningful ΔNDMI, as the high and low values of the fluctuations would negate each other. A difference in mean values could still be detected, however likely of a relatively smaller magnitude than the ΔNDMI values observed in this study. Another approach could be to only include seasonal data, to avoid the effect of fluctuations by only calculating the mean values from data points from one season, e.g. the dry season to avoid cloud cover. This would however effect data availability, and data gaps which extent the time-period used for calculating ΔNDMI, has already been observed in this study.

For the full datasets, a total accuracy of 76.3% was achieved (Table 5). The result is slightly higher than the result for the NDMI Threshold method (74.6 %). Compared to the Producer's accuracy achieved by *NDMI Threshold*, the *⊿NDMI* method was superior in detecting land cover change, without employing a threshold. A direct comparison of the accuracies achieved to previous studies is not advantageous, since no previous study based on Bfast Monitor has employed the same method framework as this study, nor for the same purpose. However, noticeable studies include DeVries et al. (2015a, 2015b), who similarly used the one-year monitoring-window sequentially iterated through-out the time-series. The studies utilized Landsat-derived NDVI, and Landsat-derived NDMI, respectively and both were conducted in tropical regions (Ethiopia and Peru). In the study in Ethiopia, 78% overall accuracy could be obtained in detecting small-scale forest disturbances based on NDVI (DeVries et al., 2015a), whereas in the study in Peru, disturbance in tropical forests could be detected with an overall accuracy of 91% based on NDMI (DeVries et al., 2015b).

The method overall performs well in the "Dense Vegetation" category as well, with an overall accuracy of 88.3% (Table 6). However the relatively lower Producer's accuracy of the "No Change" class suggests an issue in the ability of the method to not detect false breakpoints during stable land cover conditions. This is likely caused by not including a threshold in the *⊿NDMI* method. Values (very) close to zero are included in the output, however a ΔNDMI value of zero cannot represent land cover change by the definition of the ΔNDMI variable, as this suggest that there is no difference in land cover before and after the breakpoint. Since no threshold, the output is completely dependent on the breakpoints detected by the Bfast Monitor algorithm. If a false breakpoint is detected by Bfast Monitor, it will be included in the output of the ΔNDMI method, if it has a positive ΔNDMI value. To tackle this issue, a probability value was assigned to detected change pixels, as described in section 4.3.

Based on the results of the validation, it is concluded that the sensitivity of the Bfast-algorithm to outliers (causing false breakpoint detection) is also seen the *⊿NDMI* method. This issue is not further explored in this study, however a study by Schultz et al. (2016) concluded that Bfast Monitors sensitivity to outliers increases when there is little data variance in the time-series dataset. This is likely the case of the NDMI dataset (evaluated based on the visual comparison) and a consequence of studying a tropical region with a minor amount of seasonal fluctuations, compared to other geographical regions.

Overall, it can be concluded that the *⊿NDMI* method has a wider range of applicability, compared to the *NDMI Threshold*, since a threshold is not required. With further study, the output can be categorized into different types land cover change based on the corresponding ΔNDMI value of the detected breakpoints. This step could be included as a post-processing step, without adjustments to the original *⊿NDMI* method. To apply the method in other geographical regions, adjustments needs to be made in the way ΔNDMI values are calculated (e.g. due to seasonal fluctuations as discussed previously), however, compared to setting location- and vegetation-specific thresholds, this task is considered more feasible.

5.4 Performance and applicability of the automated land cover change detection method

The proposed methods in this study offer a solution to detect deforestation in tropical regions, by applying the Bfast-algorithm, without the required expert-knowledge. DeVries et al. (2015a) successfully detected small-scale forest disturbances in Ethiopia with Bfast Monitor, however with the conclusion that manual calibration of the Magnitude threshold was necessary. This restricts the application of the Bfast Monitor method by providing constraints in different locations, even locations of high similarity to their study site (DeVries et al., 2015a). The original Magnitude is somewhat comparable to ΔNDMI, in that they are both an expression of the size of a change, however defined differently. A notable difference lies in the time-periods used for calculating each parameter. The Magnitude is calculated from the entire monitoring-period while ΔNDMI is based on the year before and after the breakpoint. While the selection of included data points may be improved (e.g. according to the discussed approach, section 5.3), the ΔNDMI calculation emphasizes the difference between the land cover present before and after the breakpoint. This supports the advantage of the *ΔNDMI* method and location-specific calibration is not expected to be necessary within tropical regions. However, further testing is needed in different locations and at larger scale, due to the relatively small test-site used in this study.

5.4.1 Error sources

Additional error sources, apart from those discussed in previous sections, include the high resolution imagery accessed through Google Earth. This data was the source for selecting the study area, performing the suitability assessment of VI's and validation of the methods. Several studies have used high resolution Google Earth imagery for validation purposes (Dutrieux et al., 2016; Gutiérrez-Vélez & DeFries, 2013; Hamunyela et al., 2016), however issues exist with the accuracy of the imagery displayed. According to Google Incorporated, (2017), the date stamp on Google Earth images can be inaccurate (likely a few months or within the year stated), for several reasons, such as the true date not being reported by the image provider. Ground truth data collected manually through field work is therefore highly recommended for future validation of the methods presented in this study. To validate spatial land cover change, field observations could be collected to document recent land covers and field survey among locals could be used for historical land cover/land use data.

Other error sources which deserves attention are the effect of outliers, noise and data gaps, which have been addressed to some extent in the previous section. There can be several reasons for outliers and data gaps. Outliers can be caused by remnants of cloud and cloud shadows which were not completely removed during masking (DeVries et al., 2015a) and clouds are also likely the source of data gaps, due to extensive cloud cover in the tropics. Using Landsat ETM+ imagery further adds data gaps due to its operation in SLC-off mode from 2003 (USGS & NASA, 2003). A considerable difference in the design of the two methods exists in the respect. The *ΔNDMI* method is more sensitive to these issues since its calculation depends on a two-year period in total. However, one safeguards has been built-in against data gaps: If no data points are available in the one-year periods used to calculate ΔNDMI, no breakpoint will be recorded, even if one was detected by Bfast Monitor. Further improvement to the time period could be to remove the one-year limit, and instead base the time period on a determined number of available data point, in order to calculate the mean. The NDMI threshold is less sensitive to outliers and data gaps, with the exception of outliers which were falsely detected by Bfast Monitor as a breakpoint, and have an NDMI value below the selected threshold. Data gaps will be an issue if they occur at the actual moment of deforestation. This issue persists in remote sensing-based time-series analyses and has been addressed by a number of studies by combining data sources, such as SAR (Synthetic Aperture Radar) (Reiche et al., 2013; Reiche et al., 2015a; Reiche et al., 2015b).

5.4.2 Contribution to sustainability certification of smallholders

An automated land cover change detection method that can detect historical and near real-time deforestation in tropical regions without prior knowledge, is highly beneficial for organizations implementing certification schemes. It provides a cost-efficient method for non-experts to evaluate the sustainability of farming practices from a spatio-temporal aspect, and remote sensing tools are considered a necessity in in aiding certification processes (Scarlat & Dallemand, 2011). E.g. by providing a tool to enforce regulations regarding the cut-off date (January, 2008) defined according to ISCC requirements (ISCC, 2011). The methods proposed in this study can provide the location and timing of the establishment of investigated smallholder farms to provide documentation on if their practice was established before or after the cut-off date.

Summarizing the obtained results and discussed advantages and disadvantages, it can be concluded that the *⊿NDMI method* meets the criteria necessary (i.e. detecting SHOPPs without expert-knowledge, with the potential to be up-scaled and applied to different locations) to be a valuable tool for certification purposes. However several points needs to be addressed, before the proposed method can be implemented directly:

- Parameterization. The one-year before and after periods used to calculate the ΔNDMI of each breakpoint can be optimized for a more automatic approach to this part of the method. By extracting a certain number of data points within defined time-frames, the effect of outliers and data gaps could also be alleviated (according to the discussed approach, section 5.3).
- The robustness of the *⊿NDMI* method. According to the advantages and disadvantages, this method has potential in certification of smallholder oil palm farmers, and the focus can therefore remain on humid, tropical regions. It is still necessary to test the method in other regions of South-East Asia, as well as in the regions of South America and Africa used for oil palm cultivation and in larger areas than the 5x5 test-site.
- The probability table. With proper testing of the method, a general look up table (Figure 16) can be provided for a region, to always provide a probability map as an output. This can provide a useful post-processing tool or as a final change map without limiting the output based on ΔNDMI. An approach could be to use the same method of visual validation based on high resolution Google Earth imagery for a larger area, in order to create a representative table.
- Creating functions: The method is carried out in the open source R language and software environment. With a guiding manual the implementation can be straight forward for non-expert users, however by converting the script into a set of functions, a highly user-friendly platform can be achieved.

With attention to these points, the method can be incorporated into the certification procedures carried out by organizations, as a tool for assuring that smallholder plantations meet the defined criteria that relates to location and time of establishment.

6 Conclusions and Prospects

The main objective of this study was to detect the extent and timing of land cover conversion related to smallholder oil palm plantation establishment or expansion from multi-temporal Landsat imagery. According to a comparison performed between NDVI EVI and NDMI based on visual interpretation and a series of Bfast Monitor test-runs, this study concluded that the most suitable Landsat-derived vegetation index for this task was NDMI. An automatic approach could be developed based on the NDMI time-series, employing the Bfast-algorithm to extract the location and timing of land cover conversion related to smallholder oil palm plantation establishment. The original Bfast Monitor requires parameterization based on in-depth knowledge of the time-series data or the study area in order to correctly detect a breakpoint within the monitoring-period (DeVries et al., 2015a; Dutrieux et al., 2017). The proposed method of this study circumvents that need, by introducing an iterative framework, and selecting the most probable breakpoint by applying ΔNDMI, which is defined as the difference between the land cover present before and after the breakpoint. Finally, a probability map of the study area could be generated from the *⊿NDMI* method, showing the methods ability to correctly predict land cover change. This resulted in a minimum probability of approx. 73% for all changes detected by *⊿NDMI*.

This study showed that the Bfast Monitor could effectively identify breakpoints in Landsat time series, which could be related to land cover change. The *NDMI Threshold* and *⊿NDMI* methods obtained similar overall accuracies when evaluating against multi-temporal high-resolution Google Earth imagery, based on both the full datasets including all types of land cover change and the datasets only including deforestation. Their performance in detecting spatio-temporal deforestation caused by Smallholder Oil Palm Plantation (SHOPP) establishment, can thus be considered equal. Nevertheless, the advantages and disadvantages of each method sets them apart. In summary, the *NDMI Threshold* method has the potential of achieving high accuracies for the specific purpose of this study, if further research is conducted in setting the threshold with the most accurate outcome. The *⊿NDMI* method has potential in extending its applicability outside of the scope of this study, and can potentially achieve a probability of 100% in correctly predicting land cover change by post-processing the output.

Future research should evaluate the potential of upscaling the *⊿NDMI* method to larger areas, e.g. a Landsat scene of 170 x 185 km. As the *⊿NDMI* method considers the difference between land covers before and after the detected breakpoint, the approach would also allow detecting other land cover changes unrelated to deforestation.

In this study it has been achieved to design a promising method, which may provide a useful tool for detecting deforestation in the Riau Province, without the need for an area-specific threshold or method-specific expert-knowledge. The method is particularly beneficial for certification purposes, as the method provides both historical change detection and near real-time monitoring and therefore offers two functionalities: 1) the year and location of deforestation with an associated probability can be compared with criteria defined by certification companies e. g. the cut-off date defined by ISCC. 2) Near real-time monitoring for recent land cover development, e. g. the expansion of smallholder plantations or increasing deforestation. Finally, the method has the potential of being integrated into automated monitoring systems useful for certification organizations, since the method is developed for non-experts and uses free and open source data and software.

7 References

Asner, G. P. (2001). Cloud cover in Landsat observations of the Brazilian Amazon. *International Journal of Remote Sensing*, *22*(18), 3855–3862. https://doi.org/10.1080/01431160010006926

Bahroeny, J. J. (2009, December). Palm oil as an economic pillar of Indonesia. *The Jakarta Post*. Retrieved from http://www.thejakartapost.com/news/2009/12/02/palm-oil-economic-pillar-indonesia.html

Barry, M., Cashore, B., Clay, J., Fernandez, M., Lebel, L., Lyon, T., … Whelan, T. (2012). *Toward Sustainability: The Roles and Limitations of Certification. Executive Summary.*

Biagioni, S., Krashevska, V., Achnopha, Y., Saad, A., Sabiham, S., & Behling, H. (2015). 8000years of vegetation dynamics and environmental changes of a unique inland peat ecosystem of the Jambi Province in Central Sumatra, Indonesia. *Palaeogeography, Palaeoclimatology, Palaeoecology*, *440*, 813–829. https://doi.org/10.1016/j.palaeo.2015.09.048

Block, B. (2013). Global Palm Oil Demand Fueling Deforestation | Worldwatch Institute. Retrieved September 13, 2016, from http://www.worldwatch.org/node/6059

Broich, M., Hansen, M. C., Potapov, P., Adusei, B., Lindquist, E., & Stehman, S. V. (2011). Time-series analysis of multi-resolution optical imagery for quantifying forest cover loss in Sumatra and Kalimantan, Indonesia. *International Journal of Applied Earth Observation and Geoinformation*, *13*(2), 277–291. https://doi.org/10.1016/j.jag.2010.11.004

Cai, S., & Liu, D. (2015). Detecting Change Dates from Dense Satellite Time Series Using a Sub-Annual Change Detection Algorithm. *Remote Sensing*, *7*(7), 8705–8727. https://doi.org/10.3390/rs70708705

Carlson, K. M., Curran, L. M., Asner, G. P., Pittman, A. M., Trigg, S. N., & Marion Adeney, J. (2012). Carbon emissions from forest conversion by Kalimantan oil palm plantations. *Nature Climate Change*, *3*(3), 283–287. https://doi.org/10.1038/nclimate1702

Chen, J., Jönsson, P., Tamura, M., Gu, Z., Matsushita, B., & Eklundh, L. (2004). A simple method for reconstructing a high-quality NDVI time-series data set based on the Savitzky–Golay filter. *Remote Sensing of Environment*, *91*(3), 332–344. https://doi.org/10.1016/j.rse.2004.03.014

Cochran, W. G. (William G. (1977). *Sampling Techniques* (3rd ed.). Wiley.

Darma Tarigan, S., & Widyaliza, S. (2015). Expansion of oil palm plantations and forest cover changes in Bungo and Merangin Districts, Jambi Province, Indonesia. *Procedia Environmental Sciences*, *24*, 199–205. https://doi.org/10.1016/j.proenv.2015.03.026

DeVries, B., Decuyper, M., Verbesselt, J., Zeileis, A., Herold, M., & Joseph, S. (2015b). Tracking disturbance-regrowth dynamics in tropical forests using structural change detection and Landsat time series. *Remote Sensing of Environment*, *169*, 320–334. https://doi.org/10.1016/j.rse.2015.08.020

DeVries, B., Verbesselt, J., Kooistra, L., & Herold, M. (2015a). Robust monitoring of small-scale forest disturbances in a tropical montane forest using Landsat time series. *Remote Sensing of Environment*, *161*, 107–121. https://doi.org/10.1016/j.rse.2015.02.012

Dutrieux, L., DeVries, B., & Verbesselt, J. (2017). Introduction to BfastSpatial. Retrieved April 24, 2017, from http://www.loicdutrieux.net/bfastSpatial/#Introduction_to_bfastSpatial

Dutrieux, L. P., Jakovac, C. C., Latifah, S. H., & Kooistra, L. (2016). Reconstructing land use history from Landsat time-series: Case study of a swidden agriculture system in Brazil. *International Journal of Applied Earth Observation and Geoinformation*, *47*, 112–124. https://doi.org/10.1016/j.jag.2015.11.018

Dutrieux, L. P., Verbesselt, J., Kooistra, L., & Herold, M. (2015). Monitoring forest cover loss using multiple data streams, a case study of a tropical dry forest in Bolivia. *ISPRS Journal of Photogrammetry and Remote Sensing*, *107*, 112–125. https://doi.org/10.1016/j.isprsjprs.2015.03.015

Environmental Investigation Agency. (2014). Enforcement & monitoring needed in palm oil sector – EIA International. Retrieved May 26, 2017, from https://eia-international.org/enforcement-monitoring-needed-in-palm-oil-sector

Euler, M., Schwarze, S., Siregar, H., & Qaim, M. (2015). Oil palm expansion among smallholder farmers in Sumatra, Indonesia. *EFForTS Discussion Paper Series*, (8), 1–30. https://doi.org/2197-6244

Gaveau, D. L. A., Sheil, D., Husnayaen, Salim, M. A., Arjasakusuma, S., Ancrenaz, M., … Meijaard, E. (2016). Rapid conversions and avoided deforestation: examining four decades of industrial plantation expansion in Borneo. *Scientific Reports*, *6*, 32017. https://doi.org/10.1038/srep32017

Google Incorporated. (2017). Google Earth Help Center. Retrieved March 19, 2017, from https://support.google.com/earth

GRAS - Global Risk Assesment Services. (2015). GRAS - Land Use Change (LUC). Retrieved December 9, 2016, from https://www.gras-system.org/sustainability/land-use-change/

Gunarso, P., Hartoyo, M. E., Agus, F., & Killeen, T. J. (2013). *Oil Palm and Land Use Change in Indonesia , Malaysia and Papua New Guinea*.

Gutiérrez-Vélez, V. H., & DeFries, R. (2013). Annual multi-resolution detection of land cover conversion to oil palm in the Peruvian Amazon. *Remote Sensing of Environment*, *129*, 154–167. https://doi.org/10.1016/j.rse.2012.10.033

Hais, M., Jonášová, M., Langhammer, J., & Kučera, T. (2009). Comparison of two types of forest disturbance using multitemporal Landsat TM/ETM+ imagery and field vegetation data. *Remote Sensing of Environment*, *113*(4), 835–845. https://doi.org/10.1016/j.rse.2008.12.012

Hamunyela, E., Verbesselt, J., & Herold, M. (2016). Using spatial context to improve early detection of deforestation from Landsat time series. *Remote Sensing of Environment*, *172*, 126–138. https://doi.org/10.1016/j.rse.2015.11.006

ISCC. (2011). *ISCC 202 Sustainability Requirements for the Production of Biomass*.

ISCC. (2016). International Sustainability and Carbon Certification. Retrieved June 24, 2016, from http://www.iscc-system.org/

Jin, S., & Sader, S. A. (2005). Comparison of time series tasseled cap wetness and the normalized difference moisture index in detecting forest disturbances. *Remote Sensing of Environment*, *94*(3), 364–372. https://doi.org/10.1016/j.rse.2004.10.012

Kennedy, R. E., Yang, Z., & Cohen, W. B. (2010). Detecting trends in forest disturbance and recovery using yearly Landsat time series: 1. LandTrendr — Temporal segmentation algorithms. *Remote Sensing of Environment*, *114*(12), 2897–2910. https://doi.org/10.1016/j.rse.2010.07.008

Koh, L. P., Miettinen, J., Liew, S. C., & Ghazoul, J. (2011). Remotely sensed evidence of tropical peatland conversion to oil palm. *Proceedings of the National Academy of Sciences of the United States of America*, *108*(12), 5127–32. https://doi.org/10.1073/pnas.1018776108

Lake, R. (2016). Government to Prioritise Smallholder Mapping Via InPOP - Indonesia Palm Oil Platform. Retrieved August 25, 2016, from http://www.inpop.id/en/news/read/04-06-2016-government-to-prioritise-smallholder-mapping-via-inpop

McDonald, A. J., Gemmell, F. M., & Lewis, P. E. (1998). Investigation of the Utility of Spectral Vegetation Indices for Determining Information on Coniferous Forests. *Remote Sensing of Environment*, *66*(3), 250–272. https://doi.org/10.1016/S0034-4257(98)00057-1

Miettinen, J., Hooijer, A., Tollenaar, D., Page, S., & Malins, C. (2012). *Historical Analysis and Projection of Oil Palm Plantation Expansion on Peatland in Southeast Asia*. *Indirect Effects of Biofuel Production*.

Miettinen, J., Shi, C., & Liew, S. C. (2012). Two decades of destruction in Southeast Asia's peat swamp forests. *Frontiers in Ecology and the Environment*, *10*(3), 124–128. https://doi.org/10.1890/100236

Miettinen, J., Shi, C., & Liew, S. C. (2016). Land cover distribution in the peatlands of Peninsular Malaysia, Sumatra and Borneo in 2015 with changes since 1990. *Global Ecology and Conservation*, *6*, 67–78. https://doi.org/10.1016/j.gecco.2016.02.004

Motohka, T., Shimada, M., Uryu, Y., & Setiabudi, B. (2014). Using time series PALSAR gamma nought mosaics for automatic detection of tropical deforestation: A test study in Riau, Indonesia. *Remote Sensing of Environment*, *155*, 79–88. https://doi.org/10.1016/j.rse.2014.04.012

Nooni, I. K., Duker, A. A., Van Duren, I., Addae-Wireko, L., & Osei Jnr, E. M. (2014). Support vector machine to map oil palm in a heterogeneous environment. *International Journal of Remote Sensing*, *35*(13), 4778–4794. https://doi.org/Doi 10.1080/01431161.2014.930201

Nurdiana, A., Setiawan, Y., Pawitan, H., Prasetyo, L. B., & Permatasari, P. A. (2016). Land Changes Monitoring Using MODIS Time-series Imagery in Peat Lands Areas, Muaro Jambi, Jambi Province, Indonesia. *Procedia Environmental Sciences*, *33*, 443–449.

https://doi.org/10.1016/j.proenv.2016.03.095

Panuju, D., & Trisasongko, B. (2012). Seasonal Pattern of Vegetative Cover from NDVI Time-Series. In *Tropical Forests*. InTech. https://doi.org/10.5772/30344

Petersen, R., Aksenov, D., Esipova, E., Goldman, E., Harris, N., Kurakina, I., … Shevade, V. (2016). *Mapping tree plantations with multispectral imagery: preliminary results for seven tropical countries*. Retrieved from www.wri.org/publication/mapping-tree-plantations

Potter, C., Tan, P.-N., Steinbach, M., Klooster, S., Kumar, V., Myneni, R., & Genovese, V. (2003). Major disturbance events in terrestrial ecosystems detected using global satellite data sets. *Global Change Biology*, *9*(7), 1005–1021. https://doi.org/10.1046/j.1365-2486.2003.00648.x

Ramdani, F., & Hino, M. (2013). Land use changes and GHG emissions from tropical forest conversion by oil palm plantations in Riau Province, Indonesia. *PloS One*, *8*(7), e70323. https://doi.org/10.1371/journal.pone.0070323

Reiche, J., de Bruin, S., Hoekman, D., Verbesselt, J., & Herold, M. (2015). A Bayesian Approach to Combine Landsat and ALOS PALSAR Time Series for Near Real-Time Deforestation Detection. *Remote Sensing*, *7*(5), 4973–4996. https://doi.org/10.3390/rs70504973

Reiche, J., Souzax, C. M., Hoekman, D. H., Verbesselt, J., Persaud, H., & Herold, M. (2013). Feature Level Fusion of Multi-Temporal ALOS PALSAR and Landsat Data for Mapping and Monitoring of Tropical Deforestation and Forest Degradation. *IEEE Journal of Selected Topics in Applied Earth Observations and Remote Sensing*, *6*(5), 2159–2173. https://doi.org/10.1109/JSTARS.2013.2245101

Reiche, J., Verbesselt, J., Hoekman, D., & Herold, M. (2015). Fusing Landsat and SAR time series to detect deforestation in the tropics. *Remote Sensing of Environment*, *156*, 276–293. https://doi.org/10.1016/j.rse.2014.10.001

Rist, L., Feintrenie, L., & Levang, P. (2010). The livelihood impacts of oil palm: Smallholders in Indonesia. *Biodiversity and Conservation*, *19*(4), 1009–1024. https://doi.org/10.1007/s10531-010-9815-z

RSPO. (2016). RSPO Smallholders Definition | RSPO - Roundtable on Sustainable Palm Oil. Retrieved August 10, 2016, from https://www.rspo.org/smallholders/rspo-smallholders-definition

Sayer, J., Ghazoul, J., Nelson, P., & Klintuni Boedhihartono, A. (2012, December). Oil palm expansion transforms tropical landscapes and livelihoods. *Global Food Security*. https://doi.org/10.1016/j.gfs.2012.10.003

Scarlat, N., & Dallemand, J.-F. (2011). Recent developments of biofuels/bioenergy sustainability certification: A global overview. *Energy Policy*, *39*(3), 1630–1646. https://doi.org/10.1016/j.enpol.2010.12.039

Schultz, M., Verbesselt, J., Avitabile, V., Souza, C., & Herold, M. (2016). Error Sources in Deforestation Detection Using BFAST Monitor on Landsat Time Series Across Three Tropical Sites. *IEEE Journal of Selected Topics in Applied Earth Observations and Remote Sensing*, *9*(8), 3667–3679. https://doi.org/10.1109/JSTARS.2015.2477473

Susila, W. R., & Bourgeois, R. (2006). In the Name of Growth and Equity: The Future of Oil Palm Smallholders in Indonesia. *Moussons*, (9–10), 87–107. https://doi.org/10.4000/moussons.1981

Tan, K. T., Lee, K. T., Mohamed, A. R., & Bhatia, S. (2009). Palm oil: Addressing issues and towards sustainable development. *Renewable and Sustainable Energy Reviews*, *13*(2), 420–427. https://doi.org/10.1016/j.rser.2007.10.001

Thenkabail, P. S. (2016). *Remote sensing handbook. Volume II, Land resources monitoring, modeling, and mapping with remote sensing*. CRC Press.

Uryu, Y., Mott, C., Foead, N., Yulianto, K., Budiman, A., Takakai, F., … Stüwe, M. (2008). *Deforestation, Forest Degradation, Biodiversity Loss and CO2 Emissions in Riau, Sumatra, Indonesia*. *WWF Indonesia Technical Report*. Retrieved from http://assets.panda.org/downloads/riau_co2_report__wwf_id_27feb08_en_lr_.pdf

USGS. (2017). Product Guide: Landsat Surface Reflectance-Derived Spectral Indices.

USGS and NASA. (2003). *Preliminary Assessment of the Value of Landsat 7 ETM+ Data following Scan Line Corrector Malfunction*. Sioux Falls.

Verbesselt, J., Hyndman, R., Newnham, G., & Culvenor, D. (2010a). Detecting trend and seasonal changes in satellite image time series. *Remote Sensing of Environment*, *114*(1), 106–115. https://doi.org/10.1016/j.rse.2009.08.014

Verbesselt, J., Hyndman, R., Zeileis, A., & Culvenor, D. (2010b). Phenological change detection while accounting for abrupt and gradual trends in satellite image time series. *Remote Sensing of Environment*, *114*(12), 2970–2980. https://doi.org/10.1016/j.rse.2010.08.003

Verbesselt, J., Zeileis, A., & Herold, M. (2012). Near real-time disturbance detection using satellite image time series. *Remote Sensing of Environment*, *123*, 98–108. https://doi.org/10.1016/j.rse.2012.02.022

Verheye, W. (2010). Growth and production of oil palm. In *Land use, land cover and soil sciences*. UNESCO-EOLSS Publishers. Retrieved from https://biblio.ugent.be/publication/1009126

Viña, A., Gitelson, A. A., Nguy-Robertson, A. L., & Peng, Y. (2011). Comparison of different vegetation indices for the remote assessment of green leaf area index of crops. *Remote Sensing of Environment*, *115*(12), 3468–3478. https://doi.org/10.1016/j.rse.2011.08.010

White, M. A., & Nemani, R. R. (2006). Real-time monitoring and short-term forecasting of land surface phenology. *Remote Sensing of Environment*, *104*(1), 43–49. https://doi.org/10.1016/j.rse.2006.04.014

Wicke, B., Sikkema, R., Dornburg, V., & Faaij, A. (2011). Exploring land use changes and the role of palm oil production in Indonesia and Malaysia. *Land Use Policy*, *28*(1), 193–206. https://doi.org/10.1016/j.landusepol.2010.06.001

Wilson, E. H., & Sader, S. A. (2002). Detection of forest harvest type using multiple dates of

Landsat TM imagery. *Remote Sensing of Environment*, *80*(3), 385–396. https://doi.org/10.1016/S0034-4257(01)00318-2

Xie, Y., Sha, Z., & Yu, M. (2008). Remote sensing imagery in vegetation mapping: a review. *Journal of Plant Ecology-Uk*, *1*(1), 9–23. https://doi.org/10.1093/jpe/rtm005

Yayusman, L. F., & Nagasawa, R. (2015). ALOS-Sensor data integration for the detection of smallholder â€™ s oil palm plantation in Southern Sumatra , Indonesia, *31*(2), 27–40.

Appendix A

Mean value and standard deviation maps for Location ID1, 2006 – 2014. The time-period is limited to the imagery available in Google Earth for a direct comparison. The low mean value areas of map a) are considered likely areas of change, which corresponds to the observed land cover change in the Google Earth high resolution imagery, shown in map c) and d). The same pattern applies to the high standard deviation pixels in map b).

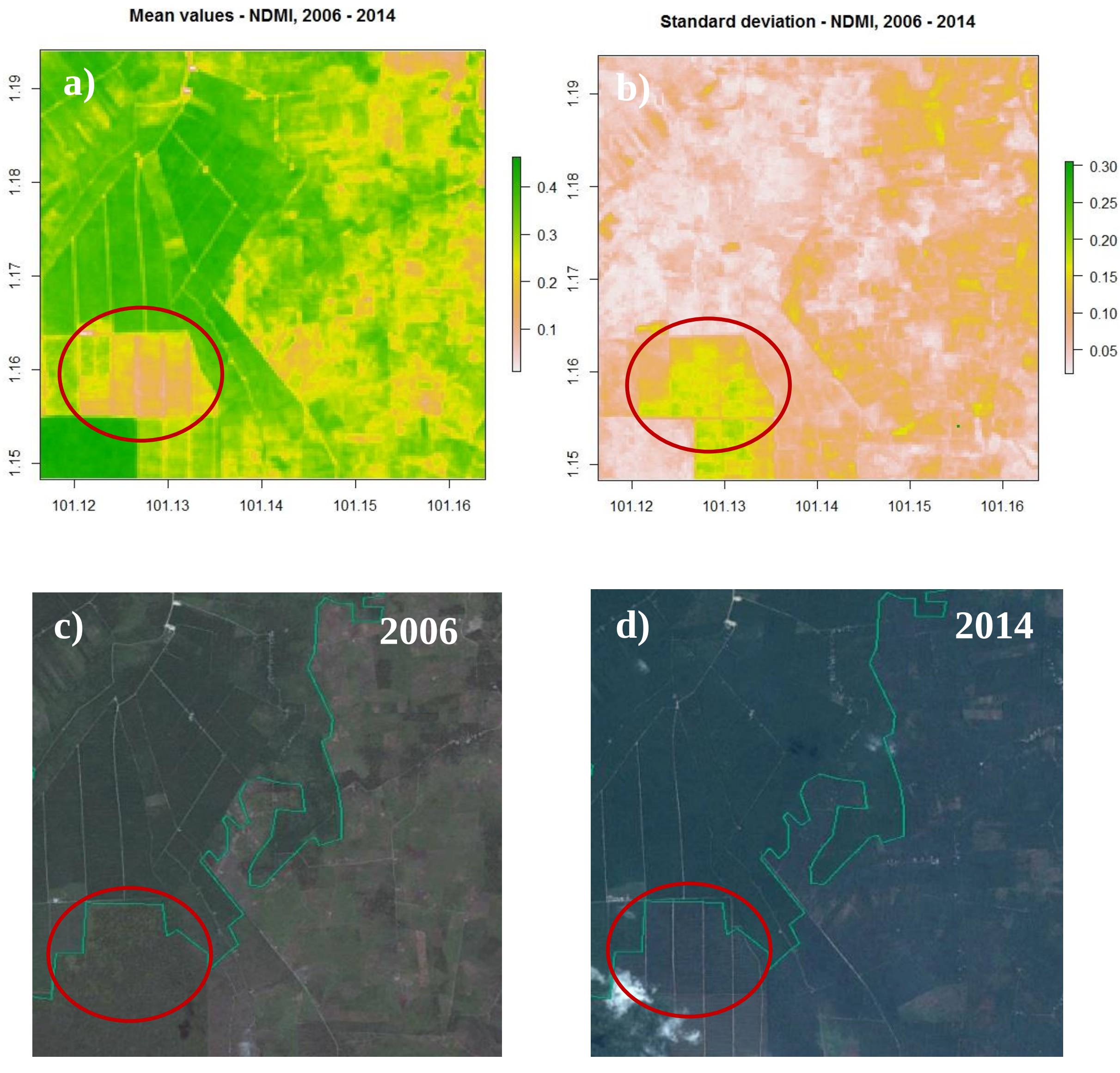

Appendix B

Calculation of the conservative and experimental NDMI threshold, based on the 100 test-pixels. First the mean NDMI of each of the test-pixels of the Stable Dense Vegetation class were found. The minimum of the mean values was chosen to represent the lower boundary of the NDMI values of stable dense vegetation, illustrated with a green line in the demonstrated time-series plot a) below. The same was done for the Stable Oil Palm class, where the minimum of the mean values was 0.38. This value was therefore considered the lower boundary for all stable vegetation. To set the lowest boundary, shown in brown in the time-series plot below, the minimum values of each raster was found. The mean of all the minimums was taken as representative of no vegetation / clearance, at -0.08. The threshold, shown in a red dashed line, was set to the mean of these two values, to fall exactly in the middle between the lower boundery of stable vegetation and the lowest boundary of no vegetation.

Calculation of threshold:

Minimum of the means of test-pixels, Stable Dense Vegetation (m_{mDV}): 0.44 NDMI

Minimum of the means of test-pixels, Stable Oil Palm (m_{mOP}): 0.38 NDMI

Means of the minimum values of all rasters of the stack (m_{mS}): - 0.08 NDMI

The likely interval where the breakpoint value may fall is then between m_{mOP} = 0.38 and m_{mS} = - 0.08. The mean between these two values are chosen as the threshold:

$NDMI_{thresh}$ (-0.08 NDMI + 0.38 NDMI) / 2 = 0.15 NDMI

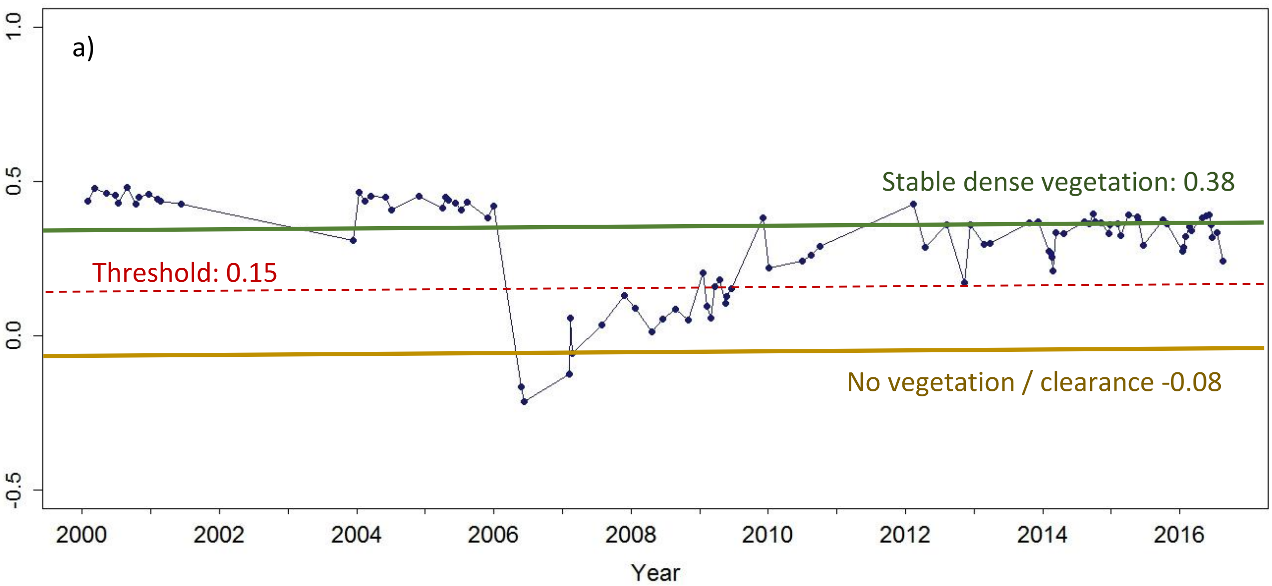

Appendix C

The spatial filter used with the spatially applied *NDMI Threshold* and *ΔNDMI* methods. The first map a) shows the output of Bfm Spatial without filter, demonstrated for the year 2013. The second map b) shows the area in hectare assigned to each pixel cluster. Pixels in all 8 directions were included as adjacent. Map c) shows the result after masking pixels below the chosen threshold.

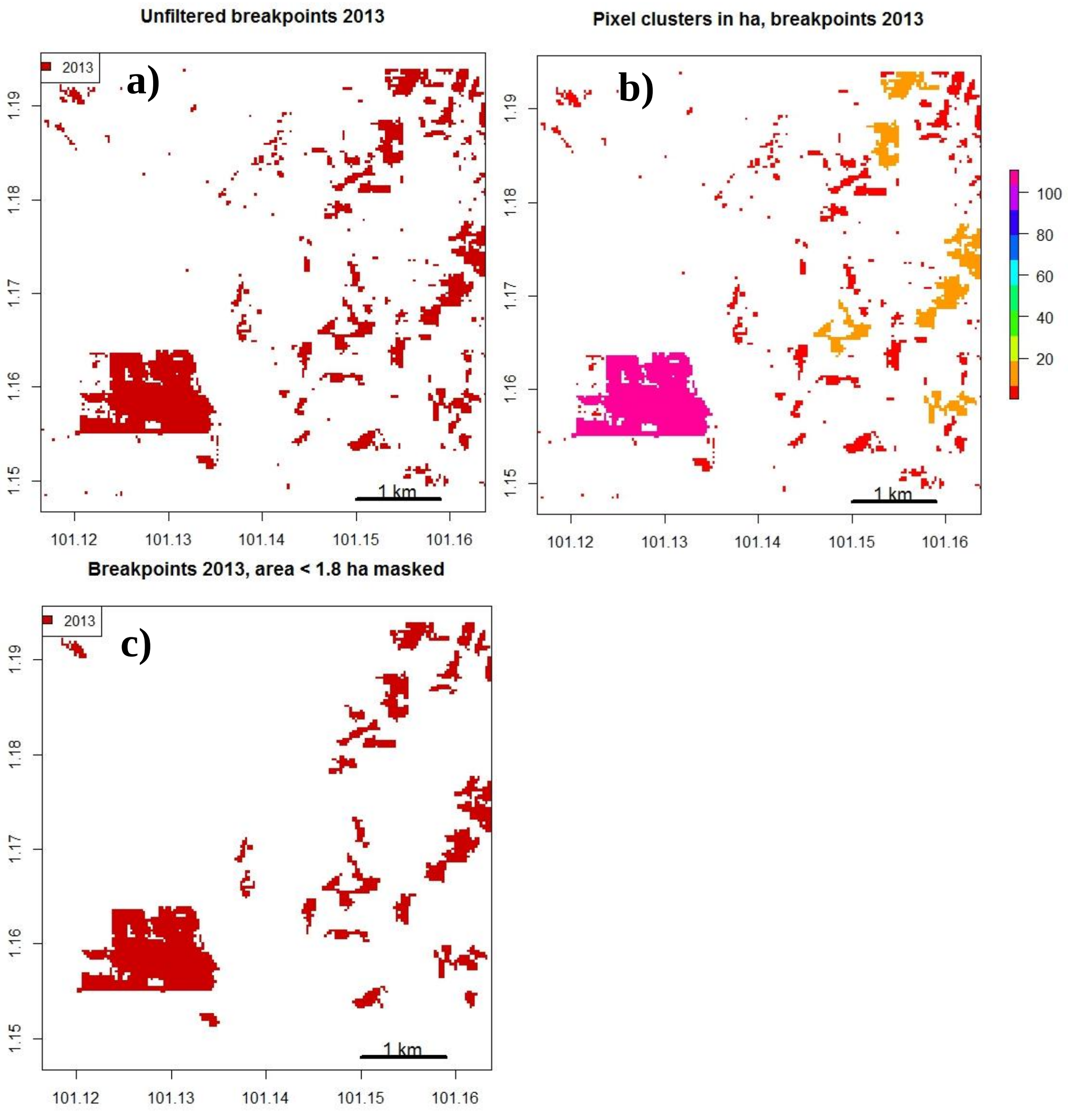

Appendix D

The script implemented in the R language and software environment. Several parts were modified from Dutrieux et al. (2017).

The following R packages were used: devtools, bfastSpatial, raster, maptools, bfast, data.table, lubridate

```
### UNZIP, EXTRACT AND CLEAN DATA ###
folder_gz <- "C:/mydir/myzippedfiles"
listzip <- list.files(folder_gz, pattern= ".tar.gz$", full.names=TRUE)

## CREATE TEMP DIRECTORY USED FOR BATCH PROCESSING
srdir <- dirout <- file.path(dirname(rasterTmpFile()), 'bfmspatial')
dir.create(dirout, showWarning=FALSE)

## RUN BATCH PROCESSING, UNZIP, EXTRACT VI AND CLOUD MASKED
output_gz <- "C:/mydir/unzippedfiles"
processLandsatBatch(x=listzip, pattern=glob2rx('*.zip'), outdir=output_gz, srdir=srdir, delete=TRUE,
vi='ndmi', mask='fmask', keep=0, overwrite=F)

### LOAD DATA AND SHOW HISTOGRAM OF SCENES ###
GRDfiles <- "C:/mydir/myGRDfiles"
listVI <- list.files(GRDfiles, pattern=glob2rx('*.grd'), full.names=TRUE)
info <- getSceneinfo(listVI)
info$year <- as.numeric(substr(info$date, 1, 4))
plot(hist(info$year, breaks=c(2000:2016), main="Scenes per Year",
   xlab="year", ylab="# of scenes"))

### CREATE RASTER BRICK ###
out_dir <- "C:/mydir"
t_stack <- file.path(out_dir, 'my_stack.grd')

Rbrick <- timeStack(x=listVI, filename=t_stack, datatype='INT2S', overwrite=TRUE)
Rbrick = calc(Rbrick, function(x) x/10000)

## CALCULATE MEAN AND STANDARD DEVIATION
meanVI <- summaryBrick(Rbrick, fun=mean, na.rm = TRUE)
stdVI <- summaryBrick(Rbrick, fun=sd, na.rm = TRUE)
meanVI_06_14 <- summaryBrick(Rbrick, fun=mean, na.rm=TRUE, minDate="2006-01-01",
                maxDate="2014-01-01")
sdVI_06_14 <- summaryBrick(Rbrick, fun=sd, na.rm=TRUE, minDate="2006-01-01",
                maxDate="2014-01-01")

### BFM PIXEL TEST RUNS ###
## load test-pixels (shapefile), Stable Dense Vegetation, Stable Oil Palm, Land Cover Change
myproj <- "+proj=longlat +datum=WGS84 +no_defs +ellps=WGS84 +towgs84=0,0,0"
pointsForest <- readShapeSpatial("C:/mydir/randompixels_forest.shp", proj4string = CRS(myproj))
```

```
## extract corresponting cellnumbers
cellNumbersForest.df <- extract(meanVI, pointsForest, cellnumber = T, df=T)
## run bfm pixel for every cell belonging to class (e.g. EVI time-series, Stable Dense Vegetation)

VI <- "EVI"
A <- NULL
B <- NULL
C <- NULL
D <- NULL
k <- 1

for (i in 1:34){
  cellID <- 1
  cell_number <- cellNumbersForest.df[cellID,2]
  bfm_cell <- bfmPixel(Rbrick, cell= cell_number, start = c(2006,1), formula = response~harmon+trend,
history = c("all"))

  nam <- paste("BfmBreak_", VI, "_", i, sep = "")
  assign(nam, bfm_cell, envir = .GlobalEnv)

  A[k] <- i
  B[k] <- cell_number
  C[k] <- bfm_cell$bfm$breakpoint
  D[k] <- nam

  k = k+1
}

total_bfm_evi <- data.frame(ID=A, Cell=B, Breakpoint=(as_date(date_decimal(C))), Name=D)
```

PIXEL BASED NDMI THRESHOLD FOR STABLE DENSE VEGETATION###

```
thresh <- 0.15

G <- NULL
H <- NULL
I <- NULL
J <- NULL
L <- NULL
K <- NULL
l <- 1

for (j in 1:34){
  cellID <- 1
  cell_number <- cellNumbersForest.df[cellID,2]

D <- NULL #breakpoint
R <- NULL #ndmi
C <- NULL #cell
```

```
Y <- NULL #year
W <- NULL #6 month index
k <- 1
for (i in 2005:2015){
  for (n in c(1,181)){

  bfmPix <- bfmPixel(Rbrick, cell=cellNum, start=c(i, n), monend = c(i+1, n), formula =
response~harmon+trend, history = c("all"), order=1)

  if (is.na(bfmPix$bfm$breakpoint) == TRUE) {

    D[k] <- NA
    R[k] <- NA
    C[k] <- cellNum
    Y[k] <- NA
    W[k] <- NA

  } else {

    out <- bfmPix$bfm$tspp

    out2 <- out[which(bfmPix$bfm$tspp$time == bfmPix$bfm$breakpoint), ]

    D[k] <- out2$time
    R[k] <- out2$response
    C[k] <- cellNum
    Y[k] <- format(date_decimal(out2$time), "%Y")
    W[k] <- n
  }
  k <- k+1
  }
}

ndmi.res <- data.frame(Breakpoint=as_date(date_decimal(D)),
                  NDMI=R, Date=Y, Index=W, Cell=C)

trueIndex <- which(ndmi.res[2] < thresh)

if (length(trueIndex) == 0L){

  G[l] <- cellNum
  I[l] <- NA
  J[l] <- NA
  K[l] <- thresh
  L[l] <- NA
  H[l] <- j

  l <- l+1

} else {
```

```
  trueBreak <- ndmi.res[trueIndex[[1]],]
  trueYear <- as.vector(trueBreak$Date)

  G[l] <- trueBreak$Cell
  I[l] <- trueYear
  J[l] <- trueBreak$NDMI
  K[l] <- thresh
  L[l] <- trueBreak$Breakpoint
  H[l] <- j

  l <- l+1
}
}

resultF <- data.frame(Cell=G, Date=I, NDMI=J, Breakpoint=L, ID=H)
```

SPATIAL NDMI THRESHOLD, e.g. 2015###

```
startMonit <- 2015
endMonit <- startMonit + 1
Smonth <- 1
dirOutput <- 'D:/mydir/NDMI 0.15'
NamePath <- file.path(dirOutput, paste(startMonit, "15_NDMI0.15.grd"))

bfmSp <- bfmSpatial(Rbrick, start = c(startMonit, Smonth), monend = c(endMonit, Smonth), formula =
response~harmon+trend, history = c("all"), overwrite=TRUE, filename = NamePath, returnLayers =
c("breakpoint"))

nam <- paste("BfmSpatial", startMonit, "_", Smonth, sep = "")
assign(nam, bfmSp, envir = .GlobalEnv)

## spatial filter
blay <- bfmSp
blayFilt <- clumpSize(blay, f=900/10000, stats = T, direction=8)
blayFilt$clumps
clumpFilt <- blayFilt$clumps
clumpFilt[blayFilt$clumps < 1.8] <- NA ## 1.8 hectares filt
Bfilt <- blay
Bfilt[is.na(clumpFilt)] <- NA

## get cell numbers
blay.df <- as.data.frame(Bfilt)
blayClean.df <- na.omit(blay.df)
blayClean.df$date <- as_date(date_decimal(blayClean.df$layer))
rnames = as.numeric(rownames(blayClean.df[1]))
NumbCell <- length(rnames)


# Apply bfm pixel to all breakpoint pixels in raster and extract NDMI
```

```
D <- NULL
R <- NULL
C <- NULL
Y <- NULL
k <- 1

for (i in 1:NumbCell){
 celln <- rnames[i]
 bfmPix <- bfmPixel(Rbrick, cell=celln, start=c(startMonit, Smonth), monend = c(endMonit, Smonth),
formula = response~harmon+trend, history = c("all"))

  out <- bfmPix$bfm$tspp
  out2 <- out[which(bfmPix$bfm$tspp$time == bfmPix$bfm$breakpoint), ]

  if (out2$response < 0.15) {
  D[k] <- out2$time
  R[k] <- out2$response
  Y[k] <- format(as_date(date_decimal(out2$time)), "%Y")
  C[k] <- tt

} else {
  print(paste(out2$time, out2$response))
}
  k <- k+1
}
ndmiVal <- data.frame(date=D,
                 ndmi=R, cell=C, Year=Y)

## create new empty raster
newR <- raster(ncol=176, nrow=169, xmn=101.1164, xmx=101.1638, ymn=1.148424, ymx=1.19397,
crs=myproj)

for (i in 1:NumbCell){
  newCell <- ndmiVal[i,3]
  newVal <- ndmiVal[i,2]

  newR[newCell] <- newVal ## how to insert new values into raster
}

## create new breakpoint layer with years
newR_2 <- raster(ncol=176, nrow=169, xmn=101.1164, xmx=101.1638, ymn=1.148424, ymx=1.19397,
crs=myproj)

for (i in 1:NumbCell){
  newCell_2 <- ndmiVal[i,3]
  newVal_2 <- as.vector(ndmiVal[i,4])

  newR_2[newCell_2] <- as.numeric(newVal_2) ## how to insert new values into raster
}
```

```
## spatial filter
NDMIlayC <- clumpSize(newR, f=900/10000, stats = T, direction=8)
NDMIFilt <- NDMIlayC$clumps
NDMIFilt[NDMIlayC$clumps < 1.8] <- NA ##
newR[is.na(NDMIFilt)] <- NA
newR_2[is.na(NDMIFilt)] <- NA

nam2 <- paste("NDMIThresh", startMonit, "_", Smonth, sep = "")
assign(nam2, newR_2, envir = .GlobalEnv)

nam3 <- paste("NDMI_values", startMonit, "_", Smonth, sep = "")
assign(nam3, newR, envir = .GlobalEnv)
```

CREATE OUTPUT FOR FULL TIME SERIES###

```
merge()
```

###PIXEL BASED ∆NDMI###

```
G <- NULL
H <- NULL
I <- NULL
J <- NULL
K <- NULL
M <- NULL
N <- NULL
l <- 1

for (i in 1:34){
cellNum <- cellNumbersBreak.df[i,2]

D <- NULL #breakpoint date
R <- NULL #past mean
V <- NULL #future mean
O <- NULL #NDMI Diff
C <- NULL #cellnumber
Y <- NULL #year
k <- 1

for (j in 2005:2015){
  for (m in c(1,181)){
  bfmPix <- bfmPixel(Rbrick, cell=cellNum, start=c(j, m), monend = c(j+1, m), formula =
response~harmon+trend, history = c("all"))
  breakpoint <- bfmPix$bfm$breakpoint
  breakpoint1 <- as_date(date_decimal(breakpoint))

 if (is.na(breakpoint1) == TRUE) {

    R[k] <- NA
    V[k] <- NA
```

```
    O[k] <- NA
    C[k] <- cellNum
    Y[k] <- NA
  } else {

    ss <- zooExtract(Rbrick, cellNum)
    ss_complete_cases <- ss[complete.cases(ss),]

    ## extract ndmi in time series corresponding to breakpoint found by bfm

    stD.p <- breakpoint1 - 90 # start date of past year
    stD.f <- breakpoint1 + 90 # start date of future year
    pastD <- stD.p - 365 # find past date after one year
    futD <- stD.f + 365 # find future date after one year

    wind.p <- window(ss, start = pastD, end = stD.p) # extract past year
    wind.p.mean <- mean(wind.p, na.rm=T) # calc mean of year
    wind.f <- window(ss, start = stD.f, end = futD) # extract future year
    wind.f.mean <- mean(wind.f, na.rm=T)

    ndmiDiff.mean <- wind.p.mean - wind.f.mean

    R[k] <- wind.p.mean
    V[k] <- wind.f.mean
    O[k] <- ndmiDiff.mean
    C[k] <- cellNum
    Y[k] <- format(as.Date(breakpoint1), "%B-%Y")

  }
  k <- k+1
  }
}

ndmi_diff <- data.frame(PastTrend=R, FutureTrend=V, Diff=O, Year=Y, Cell=C)
diff.mx <- as.matrix(ndmi_diff[3])

if (sum(diff.mx, na.rm=T)==0){

  G[l] <- cellNum
  I[l] <- NA
  J[l] <- NA
  M[l] <- NA
  N[l] <- NA
  H[l] <- i

  l <- l+1

} else {
  trueIndex <- which(ndmi_diff[3]== max(ndmi_diff[3], na.rm=T))
  trueBreak <- ndmi_diff[trueIndex[1],]
```

```
  trueYear <- as.vector(trueBreak$Year)

  G[l] <- trueBreak$Cell
  I[l] <- trueYear[1]
  J[l] <- trueBreak$Diff
  M[l] <- trueBreak$PastTrend
  N[l] <- trueBreak$FutureTrend
  H[l] <- i

  l <- l+1
}
}

resultsF <- data.frame(ID = H, Cell=G, Breakpoint=I, Diff=J, PastTrend = M, FutureTrend=N)
```

###ΔNDMI, e.g. 2005###

```
## original bfm spatial breakpoint layers were created for the full time-frame 2005-2015 in previous step
## apply spatial filter
blayFiltD <- clumpSize(bfmSp, f=900/10000, stats = T, direction=8)
clumpFiltD <- blayFiltD$clumps
clumpFiltD[blayFiltD$clumps < 1.8] <- NA
BfiltD <- bfmSp
BfiltD[is.na(clumpFiltD)] <- NA

blayD.df <- as.data.frame(BfiltD)
blayCleanD.df <- na.omit(blayD.df)
blayCleanD.df$date <- as_date(date_decimal(blayCleanD.df$layer))
rnamesD = as.numeric(rownames(blayCleanD.df[1]))
NumbCellD <- length(rnamesD)

D <- NULL #breakpoint date
O <- NULL #NDMI Diff
C <- NULL #cellnumber
Y <- NULL #year
k <- 1

for (i in 1:NumbCellD){
  cellNum <- rnamesD[i]
  BreakPD <- blayCleanD.df[i,2]

  ss <- zooExtract(Rbrick, cellNum)
  ss_complete_cases <- ss[complete.cases(ss),]

  stD.p <- BreakPD - 90 # start date of past year
  stD.f <- BreakPD + 90 # start date of future year
  pastD <- stD.p - 365 # find past date after one year
  futD <- stD.f + 365 # find future date after one year
```

```
  wind.p <- window(ss, start = pastD, end = stD.p) # extract past year
  wind.p.mean <- mean(wind.p, na.rm=T) # calc mean of year
  wind.f <- window(ss, start = stD.f, end = futD) # extract future year
  wind.f.mean <- mean(wind.f, na.rm=T)

  ndmiDiff.mean <- wind.p.mean - wind.f.mean

  D[k] <- as.character(BreakPD)
  O[k] <- ndmiDiff.mean
  C[k] <- cellNum
  Y[k] <- format(BreakPD, "%Y")

  k <- k+1
}

ndmi_Delta <- data.frame(Breakpoint=D, Diff=round(O, digits = 3), Year=Y, Cell=C)

## create new empty raster
newRD <- raster(ncol=176, nrow=169, xmn=101.1164, xmx=101.1638, ymn=1.148424, ymx=1.19397,
crs=myproj)

## create new values for raster based on breakpoint ndmi value and cellnumber
for (i in 1:NumbCellD){
  newCellD <- ndmi_Delta[i,4]
  newValD <- ndmi_Delta[i,3]
  newRD[newCellD] <- newValD ## how to insert new values into raster

}
}
```

PROBABILITY MAP

```
##Read probability table
prob.csv <- read.csv("C:/mydir/mytable.csv", header = TRUE, sep = ";",dec = ".")
prob.df <- as.data.frame(prob.csv)

P <- NULL
l <- 1

for(j in 1:NumbCellD){

  DeltaCheck <- ndmi_Delta[j,2] #diff to mach with prob

  if (is.na(DeltaCheck)){
    P[l] <- NA
  }else{

    if (DeltaCheck>=0.500){

      P[l] <- 100.0
```

```
    }else{

      if (DeltaCheck>=0){
        indexP <- which((with(prob.df,
                         start <= DeltaCheck & end >= DeltaCheck)) == TRUE)

        DProb <- prob.df[indexP,5]
        P[l] <- DProb

      }else{
        P[l] <- NA
      }
    }
  }
  l <- l+1
  print(paste(j, P[l]))
}

ndmi_Delta_Prob <- data.frame(Breakpoint=D, Diff=round(O, digits = 3), Year=Y, Cell=C, Probability=P)

## create new empty raster
newRD <- raster(ncol=176, nrow=169, xmn=101.1164, xmx=101.1638, ymn=1.148424, ymx=1.19397,
crs=myproj)

for (i in 1:NumbCellD){
  newCellD <- ndmi_Delta_Prob[i,4]
  newValD <- ndmi_Delta_Prob[i,5]
  newRD[newCellD] <- newValD
}


namProb <- paste("prob", year, "_", mon, sep = "")
assign(namProb, newRD, envir = .GlobalEnv)
```